MULTI-BOSON EFFECTS

R. LEDNICKY, V. LYUBOSHITZ, K. MIKHAILOV,
YU. SINYUKOV, A. STAVINSKY
AND B. ERAZMUS

Multi-boson effects

R. Lednický[1,2], V. Lyuboshitz[1,3], K. Mikhailov[1,4], Yu. Sinyukov[1,5],
A. Stavinsky[1,4] and B. Erazmus[1]

February 13, 1999

[1] *SUBATECH, (UMR, Université, Ecole des Mines, IN2P3/CNRS),*
4, rue Alfred Kastler, F-44070 Nantes Cedex 03, France.
[2] *Institute of Physics, Na Slovance 2, 18040 Prague 8, Czech Republic.*
[3] *JINR, 141980 Dubna, Moscow region, Russia.*
[4] *ITEP, B. Cheremushkinskaya 25, 117259 Moscow, Russia.*
[5] *ITP, Metrologicheskaya 14b, 252143 Kiev, Ukraine.*

Abstract

The influence of the multi-boson effects on pion multiplicities, single-pion spectra and two-pion correlation functions is discussed in terms of an analytically solvable model. An approximate scaling with the phase space density is demonstrated in the low density (gas) limit. This scaling and also its violation at high densities due to the condensate formation is described by approximate analytical formulae which allow, in principle, for the identification of the multi-boson effects among others. It is argued that spectacular multi-boson effects are likely to be observed only in the rare events containing sufficiently high density fluctuations.

1 Introduction

In future heavy ion experiments at RHIC and LHC one expects to obtain thousands of pions per a unit rapidity interval. Since the pions are bosons there can be multi-boson effects enhancing the production of pions with low relative momenta thus increasing the pion multiplicities, softening their spectra and modifying the correlation functions. Though the present data does not point to any spectacular multi-boson effects, one can hope to observe new interesting phenomena like boson condensation or speckles in some rare events or in eventually overpopulated kinematic regions with the pion density in the 6-dimensional phase space, $f = (2\pi)^3 d^6 n/d^3\mathbf{p}d^3\mathbf{x}$, of the order of unity (see, *e.g.*, [1]-[8]).

In the low-density limit ($f \ll 1$), the mean phase space density at a given momentum $\mathbf{p}$ can be estimated as the mean number of pions interfering with a pion of momentum $\mathbf{p}$ (rapidity y and transverse momentum $\mathbf{p}_t$) and building the Bose-Einstein (BE) enhancement in the two-pion correlation function [7, 8]: $\langle f \rangle_{\mathbf{p}} \sim \pi^{3/2} N(\mathbf{p})/V$, where $N(\mathbf{p}) = d^3 n/d^3\mathbf{p}$ and $V = r_x r_y r_z$ is the interference volume defined in terms of the outward (r_x), sideward (r_y) and longitudinal (r_z) interferometric radii. Typically $\langle f \rangle_{\mathbf{p}} \sim 0.1$ for mid-rapidities and $p_t \sim \langle p_t \rangle$ [7]. The data are also consistent with the phase space density of pions near the local thermal equilibrium [9].

At AGS and SPS energies the interference volume V seems to scale with dn/dy (see, e.g., [10, 11]) pointing to the freeze-out of the pions at a constant phase space density.[1] If this trend will survive then there will be no spectacular multi-boson effects in the ordinary events at RHIC or even at LHC. In such a situation the standard two-particle interferometry technique could be used to measure the space-time intervals between the production points also in the future collider experiments. The corresponding interferometric radii for lead-lead collisions at LHC would be however rather large - about 20 fm.

The multi-boson effects can show up however in certain classes of events. An example is a rapidly expanding system with the entropy much smaller than in the case of total equilibrium. Then a strong transversal flow can lead to rather dense gas of soft pions in the central part of the hydrodynamical tube at the final expansion stage (see, e.g., [13]). Another reason can be the formation of quark-gluon plasma or mixed phase. Due to large gradients of temperature or velocity the hydrodynamical layer near the boundary with vacuum can decay at a large phase space density and lead to pion speckles even at moderate transverse momenta [14].

The dramatic difference in behavior of Boltzmann-like gases and dense multi-boson systems can lead to serious problems for transport models like RQMD, VENUS, etc., ignoring actually the statistical properties of the particles both in intermediate and final states. In these models the most intensive particle production happens at relatively early evolution (expansion) stage when rather large pion phase space densities can be achieved at RHIC or LHC energies.

Generally, the account of the multi-boson effects is extremely difficult task. Even on the neglection of particle interaction in the final state the requirement of the BE symmetrization leads to severe numerical problems which increase factorially with the number of produced bosons [3, 4]. In such a situation, it is important that there exists a simple analytically solvable model [5] allowing for a study of the characteristic features of the multi-boson systems under various conditions including those near the Bose condensation. In this paper we use this model to demonstrate the influence of the multi-boson effects on pion multiplicities, spectra and two-pion correlation functions. Besides the original papers [5, 6], similar studies can be found also in [15, 16, 17]. Particularly, some of the new aspects of the multi-boson effects, like the scaling behavior with the phase space density or the behavior of the (semi-)inclusive correlation functions near the condensation limit were studied in our unpublished paper [15]. The present work represents an elaborated version of the latter.

In Section 2 we introduce the space-time description of particle production in terms of Wigner-like densities and discuss their physical meaning and the conditions of their factorization in the model of classical one-particle sources. The multi-boson formalism in the factorizable case is set forth in Section 3. Using this formalism and the simple Gaussian ansatz for the emission function, we present in Section 4 the analytical solutions (partly in terms of the recurrence relations) for the multiplicity distribution, single-boson spectra and two-boson correlation functions. In Section 5 we compare the results of numerical calculations with the analytical approximations accounting for the approximate scaling behavior in the low density (gas) limit as well as for the condensate formation at high densities. The results are discussed and summarized in Section 6.

---

[1]Similar effect was observed also for protons produced in hadron- and electron-nucleus interactions [12].

2 Space-time picture of particle production

2.1 Wigner-like density

Let us first consider a process in which, besides others, just n non-identical particles of given types are produced with the 4-momenta $p_i = \{E_i, \mathbf{p}_i\}$ and Lorentz factors $\gamma_i = E_i/m_i$ (to simplify the notation, we assume that particles are spinless). The inclusive differential cross section of this process is described by the invariant production amplitude $T_n(p_1, \ldots, p_n; \alpha)$:

$$\gamma_1 \cdots \gamma_n \frac{d^{3n}\sigma_n}{d^3\mathbf{p}_1 \cdots d^3\mathbf{p}_n} = \sum_\alpha \mid T_n(p_1, \ldots, p_n; \alpha) \mid^2 \equiv \gamma_1 \cdots \gamma_n \sigma_n P_n(\mathbf{p}_1, \ldots, \mathbf{p}_n), \quad (1)$$

where the sum over the quantum numbers α, describing the rest of the produced system, contains also an integration over the momenta of the other produced particles with the energy-momentum conservation taken into account. The non-invariant production probability P_n is normalized to unity as:

$$\int d^3\mathbf{p}_1 \cdots d^3\mathbf{p}_n P_n(\mathbf{p}_1, \ldots, \mathbf{p}_n) = 1. \quad (2)$$

If the particles are identical spinless bosons, then the production amplitude has to satisfy the requirement of Bose symmetry. Formally, this can be achieved by the substitution of the non-symmetrized amplitude $T_n(p_1, \ldots, p_n; \alpha)$ (corresponding to the "switched off" effect of quantum statistics) by a properly symmetrized one:

$$T_n(p_1, \ldots, p_n; \alpha) \to (n!)^{-1/2} \sum_\sigma T_n(p_{\sigma_1}, \ldots, p_{\sigma_n}; \alpha), \quad (3)$$

where the sum is over all $n!$ permutations σ of the sequence $\{1, 2, \ldots n\}$.

In the following we will neglect particle interaction in the final state.[2] Then the non-symmetrized amplitude $T_n(p_1, \ldots, p_n; \alpha)$ is related to the amplitude in the space-time representation $\mathcal{T}_n(x_1, \ldots, x_n; \alpha)$ (describing production of the particles in the space-time points with the 4-coordinates $x_1, \ldots, x_n$) by the usual Fourier transform:

$$T_n(p_1, \ldots, p_n; \alpha) = \int d^4x_1 \ldots d^4x_n e^{ip_1 x_1 + \cdots ip_n x_n} \mathcal{T}_n(x_1, \ldots, x_n; \alpha). \quad (4)$$

Inserting (4) into (1) and introducing the space-time density matrix [19]:

$$\rho_n(x_1, \ldots, x; x_1', \ldots, x_n') = \sum_\alpha \mathcal{T}_n(x_1, \ldots, x_n; \alpha) \mathcal{T}_n^*(x_1', \ldots, x_n'; \alpha) \quad (5)$$

and its partial Fourier transform (emission function) - an analogy of the Wigner density [20]:

$$\widetilde{D}_n(p_1, \bar{x}_1; \ldots; p_n, \bar{x}_n) \equiv \gamma_1 \cdots \gamma_n \sigma_n D_n(p_1, \bar{x}_1; \ldots; p_n, \bar{x}_n)$$

$$= \int d^4\delta_1 d^4\delta_2 e^{ip_1\delta_1 + \cdots ip_n\delta_n} \rho_n(\bar{x}_1 + \tfrac{1}{2}\delta_1, \ldots, \bar{x}_n + \tfrac{1}{2}\delta_n; \bar{x}_1 - \tfrac{1}{2}\delta_1, \ldots, \bar{x}_n - \tfrac{1}{2}\delta_n), \quad (6)$$

---

[2]This is more or less valid assumption for neutral pions but not for the charged ones. For the treatment of multi-boson effects in the case of interacting pions see, e.g., [18].

3

where $\bar{x}_i = \frac{1}{2}(x_i + x_i')$, $\delta_i = x_i - x_i'$, we can rewrite the production cross section (1) in the absence of BE effects as:

$$\frac{d^{3n}\sigma_n}{d^3\mathbf{p}_1 \cdots d^3\mathbf{p}_n} \equiv \sigma_n P_n(\mathbf{p}_1, \ldots, \mathbf{p}_n) = \sigma_n \int d^4\bar{x}_1 \cdots d^4\bar{x}_n D_n(p_1, \bar{x}_1; \ldots; p_n, \bar{x}_n). \quad (7)$$

Since D_n is a real (though not positively defined) function normalized to unity, in accordance with Eq. (7) it can be considered as an approximation to the emission probability of the particles with given 4-momenta p_i in the average space-time points $\bar{x}_i = \frac{1}{2}(x_i + x_i')$.

The insertion of the symmetrized amplitude (3) into the cross section formula (1) leads to the substitution of the probability P_n by a BE modified one P_n^c. For example, in the case of a two-boson production process, instead of Eq. (7) we have:

$$P_2^c(\mathbf{p}_1, \mathbf{p}_2) = \int d^4x_1 d^4x_2 [D_2(p_1, x_1; p_2, x_2) + D_2(p, x_1; p, x_2)\cos(qx)], \quad (8)$$

where $p = \frac{1}{2}(p_1 + p_2)$, $q = p_1 - p_2$ and $x = x_1 - x_2$. Clearly, for $n > 1$ the probability P_n^c is no more normalized to unity. The integral over this probability yields the BE weight ω_n of an n-boson event produced in the absence of the effect of quantum statistics ($\omega_0 = \omega_1 = 1$, $\omega_n > 1$ for $n > 1$):

$$\int d^3\mathbf{p}_1 \cdots d^3\mathbf{p}_n P_n^c(\mathbf{p}_1, \ldots, \mathbf{p}_n) = \omega_n. \quad (9)$$

We will also use the differential BE weights defined as

$$\omega_n^{(k)}(\mathbf{p}_1, \ldots, \mathbf{p}_k) = \frac{\int d^3\mathbf{p}_{k+1} \cdots d^3\mathbf{p}_n P_n^c(\mathbf{p}_1, \ldots, \mathbf{p}_k, \ldots, \mathbf{p}_n)}{\int d^3\mathbf{p}_{k+1} \cdots d^3\mathbf{p}_n P_n(\mathbf{p}_1, \ldots, \mathbf{p}_k, \ldots, \mathbf{p}_n)}. \quad (10)$$

The multi-boson problem greatly simplifies (see Section 3) in the factorizable case when the n-particle emission function and, as a consequence, the non-symmetrized production probability can be written as products of the single-particle ones:

$$D_n(p_1, x_1; \ldots; p_n, x_n) = D(p_1, x_1) \cdots D(p_n, x_n), \quad P_n(\mathbf{p}_1, \ldots, \mathbf{p}_n) = P(\mathbf{p}_1) \cdots P(\mathbf{p}_n). \quad (11)$$

Consequently, the BE weights are expressed through a universal function F_{ij} (see, e.g., [18]):

$$\omega_n^{(n)}(\mathbf{p}_1, \mathbf{p}_2, \ldots \mathbf{p}_n) = \sum_{\sigma} \prod_{i=1}^{n} F_{i\sigma_i}, \quad (12)$$

where

$$F_{ij} = \int d^4x D(p_{ij}, x) \cdot \exp(iq_{ij}x) / [P(\mathbf{p}_i)P(\mathbf{p}_j)]^{1/2}, \quad (13)$$

$p_{ij} = \frac{1}{2}(p_i + p_j)$ and $q_{ij} = p_i - p_j$. The sum in Eq. (12) is over $n!$ possible permutations σ of the sequence $\{1, 2, \ldots n\}$. For example, in the two-boson case, we have

$$\omega_2^{(2)}(\mathbf{p}_1, \mathbf{p}_2) = F_{11}F_{22} + F_{12}F_{21} \equiv 1 + K_2^{(2)}(\mathbf{p}_1, \mathbf{p}_2), \quad (14)$$

where $K_2^{(2)} = F_{12}F_{21}$ is so called differential cumulant (see Section 3).

4

2.2 One-particle sources

To clarify the physical meaning of the emission function and the factorization assumption (11), let us follow Kopylov and Podgoretsky (see, *e.g.*, [1]) and assume that particles $1, 2, \ldots$ are emitted by one-particle sources $A, B, \ldots$ which are considered as classical so they can be treated by parameters and not by amplitudes. Thus the 4-coordinates of the source centers $x_A, x_B, \ldots$ and other source characteristics in the model can be considered as a part of the quantum numbers $\alpha \equiv \{x_A, x_B, \ldots \alpha'\}$. It was pointed out by Kopylov and Podgoretsky that the BE effect is mainly determined by the phase factor $\exp(ip_1 x_A + ip_2 x_B + \cdots)$ contained in the amplitude $T_n(p_1, \ldots, p_n; \alpha)$.

Let us first consider the production of only one boson. Assuming the translation invariance of the decay amplitudes $\tilde{u}$, we can write the single-boson amplitude in the 4-coordinate representation as:

$$\mathcal{T}(x_1; \alpha) \equiv \tilde{t}(x_1 - x_A; \alpha) = \tilde{u}(x_1 - x_A; \alpha')v(\alpha), \tag{15}$$

where $\alpha = \{x_A, \alpha'\}$ and $\alpha' = \{A, \ldots\}$. Inserting (15) into (4) and introducing the Fourier transform

$$t(p; \alpha) = \int d^4\xi e^{ip\xi}\tilde{t}(\xi; \alpha) \equiv u(p; \alpha')v(\alpha), \tag{16}$$

we obtain the Kopylov-Podgoretsky ansatz:

$$T(p; \alpha) = e^{ipx_A}t(p; \alpha) \equiv e^{ipx_A}u(p; \alpha')v(\alpha). \tag{17}$$

For the production probability we have

$$P^c(\mathbf{p}) = P(\mathbf{p}) \equiv \int d^4x_A W(p, x_A) = \int d^4x_A \sum_{\alpha'} |t(p; \{x_A, \alpha'\})|^2, \tag{18}$$

where we have introduced the (true) emission probability $W(\mathbf{p}, x_A)$. Similarly, if two bosons are produced, the production probability takes on the form:

$$P_2^c(\mathbf{p}_1, \mathbf{p}_2) = \int d^4x_A d^4x_B \sum_{\alpha'} \{|t(p_1, p_2; \alpha)|^2 + Re[t(p_1, p_2; \alpha)t^*(p_2, p_1; \alpha)e^{iqx}]\}. \tag{19}$$

Note that here $x = x_A - x_B$ and, as usual, $q = p_1 - p_2$.

The emission function D can be expressed through the Kopylov-Podgoretsky amplitudes $t(p; \alpha)$ continued off mass-shell. Substituting Eq. (15) into Eq. (5) and using the inverted Fourier transform in Eq. (16), we get from Eq. (6) [18]:

$$\begin{aligned} D(p, \bar{x}_1) &= \tfrac{1}{(2\pi)^4} \sum_{\alpha'} \int d^4x_A d^4\kappa e^{i\kappa(x_A - \bar{x}_1)} \cdot t(p + \tfrac{1}{2}\kappa; \{x_A, \alpha'\})t^*(p - \tfrac{1}{2}\kappa; \{x_A, \alpha'\}) \\ &= \tfrac{1}{(2\pi)^4} \sum_{\alpha'} \int d^4x_A d^4\kappa e^{i\kappa(x_A - \bar{x}_1)} \cdot u(p + \tfrac{1}{2}\kappa; \alpha')u^*(p - \tfrac{1}{2}\kappa; \alpha')|v(\alpha)|^2. \end{aligned} \tag{20}$$

It is clear from Eq. (16) that the momentum dependence of the amplitude $t(p; \alpha)$ is determined by the space-time extent of the one-particle source. For example, assuming that the source emits a particle independently of the quantum numbers α' except for the source type A: $\tilde{u}(\xi; \alpha') = \tilde{u}(\xi; A)$ and that the distribution of the emission points in the source rest frame is given by a simple Gaussian

$$\tilde{u}(\xi; A) \sim \exp(-\frac{\boldsymbol{\xi}^2}{2r_A^2} - \frac{\xi_0^2}{2\tau_A^2}), \tag{21}$$

5

the parameters r_A and τ_A characterizing the proper space-time sizes of the source A, we obtain in the case of a source at rest:[3]

$$t(p; \alpha) \sim \exp(-\frac{1}{2}r_A^2 \mathbf{p}^2 - \frac{1}{2}\tau_A^2 p_0^2)v(\alpha). \tag{22}$$

The probability $|v(\alpha)|^2$ describes the production of particle sources and depends on the 4-coordinates x_A of the source centers. In the following we will take it also in a simple Gaussian form:

$$|v(\alpha)|^2 \sim \exp(-\frac{\boldsymbol{x}_A^2}{2\tilde{r}_0^2} - \frac{x_{0A}^2}{2\tilde{\tau}_0^2}), \tag{23}$$

where the parameters $\tilde{r}_0$ and $\tilde{\tau}_0$ characterize the space-time distribution of the sources.

Comparing Eqs. (18) and (20), it can be seen that the emission function D is more spread in space and time than the emission probability W. In particular, the Gaussian parametrizations in Eqs. (21) and (23) yield:

$$W(p, x) \sim \exp(-r_A^2 \mathbf{p}^2 - \tau_A^2 p_0^2) \exp(-\frac{\mathbf{x}^2}{2\tilde{r}_0^2} - \frac{x_0^2}{2\tilde{\tau}_0^2}) \tag{24}$$

and

$$D(p, x) \sim \exp(-r_A^2 \mathbf{p}^2 - \tau_A^2 p_0^2) \exp(-\frac{\mathbf{x}^2}{2\tilde{r}_0^2 + r_A^2} - \frac{x_0^2}{2\tilde{\tau}_0^2 + \tau_A^2}). \tag{25}$$

In the case of independent one-particle sources characterized by the same parameters and on the condition of a negligible relative motion of the sources (to avoid the modification of the decay amplitudes due to the Doppler shifts), the emission function takes on the factorized form as in Eq. (11). We then get, for example, in the two-boson case (see Eq. (8)):

$$P_2^c(\mathbf{p}_1, \mathbf{p}_2) = P(\mathbf{p}_1)P(\mathbf{p}_2)[1 + \exp(-\tilde{r}_0^2 \mathbf{q}^2 - \tilde{\tau}_0^2 q_0^2)]. \tag{26}$$

It is interesting to note, that in this factorizable case the BE correlation effect is determined solely by the characteristic space-time distance between the centers of the one-particle sources. In terms of the Kopylov-Podgoretsky emission amplitudes, this result immediately follows from Eq. (19), or directly, from Eqs. (1) and (3).

The space-time extent of the one-particle sources can be usually considered much smaller than the characteristic space-time distance between their centers ($r_A \ll \tilde{r}_0$, $\tau_A \ll \tilde{\tau}_0$). The 4-momentum dependence of the one-particle amplitudes is then negligible when varying the particle 4-momenta by the amount $\sim \tilde{r}_0^{-1}, \tilde{\tau}_0^{-1}$ characteristic for the interference effect. On such a *smoothness* condition there is practically no difference between the emission function D and the emission probability W and both Eqs. (8) and (19) yield the well known result of Kopylov-Podgoretsky for the production probability of two identical bosons:

$$P_2^c(\mathbf{p}_1, \mathbf{p}_2) \doteq P(\mathbf{p}_1, \mathbf{p}_2)[1 + \langle\cos(q(x_1 - x_2))\rangle]. \tag{27}$$

---

[3]Note that Eq. (22) is valid also off mass-shell when $p_0 \neq E$.

6

3 Multi-boson formalism in the factorizable case

The multi-boson effects can be practically treated provided that we can neglect particle interaction in the final state and assume independent emission of non-interfering particles (a valid assumption for heavy ion collisions), supplemented by the requirement of a universal single-particle emission function $D(p, x)$, independent of the origin of single-particle sources. We can then use Eq. (11) expressing the n-particle emission function as a product of the single-particle ones. Then, similar to refs. [5, 6] it is convenient to define the functions

$$
\begin{aligned}
G_1(\mathbf{p}_1, \mathbf{p}_2) &= \int d^4 x\, D(\tfrac{1}{2}(p_1 + p_2), x) \cdot \exp(i(p_1 - p_2)x), \\
G_n(\mathbf{p}_1, \mathbf{p}_2) &= \int d^3 k_2 \ldots d^3 k_n G_1(\mathbf{p}_1, \mathbf{k}_2) \ldots G_1(\mathbf{k}_n, \mathbf{p}_2) \\
&\equiv \int d^3 k_2 G_{n-1}(\mathbf{p}_1, \mathbf{k}_2) G_1(\mathbf{k}_2, \mathbf{p}_2), \\
g_n &= \int d^3 p\, G_n(\mathbf{p}, \mathbf{p}).
\end{aligned}
\tag{28}
$$

The function G_1 at equal momenta is just the original (not affected by the multi-boson effects) single-boson spectrum normalized to unity:

$$
P(\mathbf{p}) = G_1(\mathbf{p}, \mathbf{p}), \quad \int d^3 p\, P(\mathbf{p}) \equiv g_1 = 1.
\tag{29}
$$

The related quantities are so called cumulants

$$
\begin{aligned}
K_n^{(2)}(\mathbf{p}_1, \mathbf{p}_2) &= (n - 2)! \sum_{i=1}^{n-1} G_i(\mathbf{p}_1, \mathbf{p}_2) G_{n-i}(\mathbf{p}_2, \mathbf{p}_1) \,/\, [P(\mathbf{p}_1) P(\mathbf{p}_2)], \\
K_n^{(1)}(\mathbf{p}) &= (n - 1)! G_n(\mathbf{p}, \mathbf{p}) \,/\, P(\mathbf{p}), \\
K_n &= (n - 1)! g_n.
\end{aligned}
\tag{30}
$$

It can be shown that the BE weight of an event with n identical spin-zero bosons is determined through the cumulants K_j by the recurrence relation [18]:

$$
\omega_n = C_0^{n-1} K_1 \omega_{n-1} + C_1^{n-1} K_2 \omega_{n-2} + \ldots + C_{n-1}^{n-1} K_n \omega_0
\tag{31}
$$

with $\omega_0 = \omega_1 = 1$; $C_i^{n-1} = (n - 1)!/[i!(n - 1 - i)!]$ are the usual combinatorial numbers. For example, $\omega_2 = 1 + K_2$ and $\omega_3 = 1 + 3K_2 + K_3$. One can check that $\omega_n = n!$ provided that all the elementary one-particle sources are situated at one and the same space-time point so that all the single-boson states are identical and $K_{j+1} = j!$.[4] In the other extreme case of a large phase space volume and $n^2 K_2 \ll 1$, we can neglect the contribution of the higher order cumulants except for the first power of K_2 and write:

$$
\omega_n \doteq 1 + C_2^n K_2.
\tag{32}
$$

---

[4]This situation is similar (flat correlation function) though different from the case of the emission of so called coherent bosons for which there is no enhancement factor. In fact, when the one-particle sources become closer and closer, so that their distances are less than the wave length of the emitted bosons, they can no more be considered as independent ones and a multi-particle source of non-interfering bosons has to be introduced [21]. To quantify the transition to the non-interfering bosons a concept of the coherence length can be used [22].

Given the original multiplicity distribution $\widetilde{w}(n)$, the BE affected one is easily calculated using the BE weights ω_n:

$$w(n) = \omega_n \widetilde{w}(n) \Big/ \sum_{j=0}^{\infty} \widetilde{w}(j). \tag{33}$$

Particularly, assuming the original Poissonian distribution with the mean multiplicity η: $\widetilde{w}(n) = e^{-\eta}\eta^n/n!$, we get:

$$w(n) = \omega_n \frac{\eta^n}{n!} \Big/ \sum_{j=0}^{\infty} \omega_j \frac{\eta^j}{j!}. \tag{34}$$

Similarly, the BE affected single- and two-boson spectra, respectively normalized to n and $n(n-1)$, can be written as

$$N_n^{(1)}(\mathbf{p}) \equiv N_n(\mathbf{p}) = n\omega_n^{(1)}(\mathbf{p}) \cdot P(\mathbf{p}) \,/\, \omega_n \tag{35}$$

and

$$N_n^{(2)}(\mathbf{p}_1, \mathbf{p}_2) = n(n-1)\omega_n^{(2)}(\mathbf{p}_1, \mathbf{p}_2)P(\mathbf{p}_1)P(\mathbf{p}_2) \,/\, \omega_n, \tag{36}$$

where the differential BE weights $\omega_n^{(1)}(\mathbf{p})$ and $\omega_n^{(2)}(\mathbf{p}_1, \mathbf{p}_2)$ are expressed through the differential cumulants $K_n^{(1)}(\mathbf{p})$ and $K_n^{(2)}(\mathbf{p}_1, \mathbf{p}_2)$ [15]:

$$\omega_n^{(1)}(\mathbf{p}) \equiv \int d^3\mathbf{p}' \omega_n^{(2)}(\mathbf{p}, \mathbf{p}')P(\mathbf{p}') = \sum_{j=0}^{n-1} C_j^{n-1} K_{j+1}^{(1)}(\mathbf{p})\omega_{n-1-j},$$

$$\omega_n^{(2)}(\mathbf{p}_1, \mathbf{p}_2) = \sum_{j=0}^{n-2} C_j^{n-2}\omega_{n-2-j}\left[\sum_{l=0}^{j} C_l^j K_{l+1}^{(1)}(\mathbf{p}_1)K_{j-l+1}^{(1)}(\mathbf{p}_2) + K_{j+2}^{(2)}(\mathbf{p}_1, \mathbf{p}_2)\right]. \tag{37}$$

The differential weight $\omega_n^{(2)}(\mathbf{p}_1, \mathbf{p}_2)$ can be considered as a two-particle correlation function measuring the BE effect on the original uncorrelated two-particle spectrum $\widetilde{N}_n^{(2)}(\mathbf{p}_1, \mathbf{p}_2) = n(n-1)P(\mathbf{p}_1)P(\mathbf{p}_2)$, with the normalization

$$\int d^3\mathbf{p}_1 d^3\mathbf{p}_2 \omega_n^{(2)}(\mathbf{p}_1, \mathbf{p}_2)P(\mathbf{p}_1)P(\mathbf{p}_2) = \omega_n. \tag{38}$$

Usually the correlation function is normalized to unity at a large $|\mathbf{q}|$. Such a normalization is approximately satisfied for the correlation function defined as:

$$R_n(\mathbf{p}_1, \mathbf{p}_2) = N_n^{(2)}(\mathbf{p}_1, \mathbf{p}_2) \,/\, \widetilde{N}_n^{(2)}(\mathbf{p}_1, \mathbf{p}_2) \equiv \omega_n^{(2)}(\mathbf{p}_1, \mathbf{p}_2) \,/\, \omega_n. \tag{39}$$

In practice, the two-particle correlation function is defined through the observable spectra as:

$$R_n(\mathbf{p}_1, \mathbf{p}_2) = c_n N_n^{(2)}(\mathbf{p}_1, \mathbf{p}_2) \,/\, [N_n^{(1)}(\mathbf{p}_1)N_n^{(1)}(\mathbf{p}_2)]. \tag{40}$$

Similarly, the (semi-)inclusive correlation function is defined as

$$R(\mathbf{p}_1, \mathbf{p}_2) = c \, N^{(2)}(\mathbf{p}_1, \mathbf{p}_2) \,/\, [N^{(1)}(\mathbf{p}_1)N^{(1)}(\mathbf{p}_2)], \tag{41}$$

where

$$N^{(1)}(\mathbf{p}) = \sum_n w(n)N_n^{(1)}(\mathbf{p}), \qquad N^{(2)}(\mathbf{p}_1, \mathbf{p}_2) = \sum_n w(n)N_n^{(2)}(\mathbf{p}_1, \mathbf{p}_2) \tag{42}$$

are the corresponding (semi-)inclusive single- and two-particle spectra, $w(n)$ is the normalized multiplicity distribution accounting for the BE effect according to Eq. (33). Later on, using an analytical Gaussian model for the emission function, we show that the normalization constant c_n can be expressed through the BE weights as:

$$c_n = n\omega_{n-1}^2 \, / \, [(n-1)\omega_n \omega_{n-2}] \tag{43}$$

and that $c = 1$ for the inclusive correlation function provided a Poissonian multiplicity distribution of the original uncorrelated bosons.

As one can see from formulae (35)-(37), the multi-boson correlations lead to distortions of the original single- and two-particle distributions. Such distortions are small in the case of interference of only two or three identical particles. However, they can become essential for the events with a large number of identical bosons due to factorially increasing number of the correction terms [3] (see also [1] and [5]). For the processes characterized by a high (> 0.1) phase space density of the identical bosons at the freeze-out time the multi-boson effects can no more be considered as a correction [3].

To account for the multi-boson symmetrization effect in the event simulators, a phase space weighting procedure was used with weights in the form of a normalized square of the sum of $n!$ plane waves [3, 4]. This procedure however appears not practical for a large n due to the factorially large number of the terms to be computed to calculate the weight and, due to large weight fluctuations. These fluctuations can be substantially reduced by weighting only in the momentum space. The corresponding BE weights are given in Eq. (12). They are expressed through the universal function (13) which is simply related with the function G_1:

$$F_{ij} = G_1(\mathbf{p}_i, \mathbf{p}_j) \, / \, [P(\mathbf{p}_i)P(\mathbf{p}_j)]^{1/2}. \tag{44}$$

On the condition of sufficient smoothness of the single-particle spectra, we can put

$$F_{ij} \doteq \int d^4x D(p_{ij}, x) \cdot \exp(iq_{ij}x) \, / \int d^4x D(p_{ij}, x), \tag{45}$$

where $p_{ij} = \frac{1}{2}(p_i + p_j)$ and $q_{ij} = p_i - p_j$. This function can then be calculated as suggested in [18]:

$$F_{ij} = \langle \exp(iq_{ij}x_k) \rangle_{\mathbf{p}_{ij}}, \tag{46}$$

where the averaging is done over all simulated phase space points $\{p_k, x_k\}$ such that $\mathbf{p}_k$ is close to a given 3-momentum $\mathbf{p}_{ij}$. However, there is still the problem with factorially large number of the terms required to calculate the weight according to Eq. (12).

Fortunately, when calculating only single- or two-particle distributions according to Eqs. (35) or (36), this number is strongly reduced (eaten by the combinatorial numbers C_j^m in Eqs. (37)). We should however perform integration over momenta of one or more particles to determine the integrated cumulants $K_n^{(2)}(\mathbf{p}_1, \mathbf{p}_2)$, $K_n^{(1)}(\mathbf{p})$ and K_n.

The numerical averaging of the cumulants of all orders is a difficult task. In the case of large multiplicities of identical bosons ($n > 20$) this is practically possible in the models with a symmetric emission function (allowing to use a special Monte Carlo technique) [3] or with a simple analytical parametrization of this function [5, 6]. For example, in ref. [6] the corrections to multiplicity distributions, single-particle spectra and two-particle correlation functions were calculated using the relativistic Bjorken model [23] for the emission function. To compute cumulants up to tenth order, the integration was performed analytically over the space-time coordinates and numerically over the momenta.

Generally, for realistic models used to predict particle production in ultra-relativistic heavy-ion collisions, the numerical limitations allow to determine only a few lowest order cumulants (up to about the fourth order) [18]. Fortunately, since the interferometry measurements point out to a moderate pion freeze-out phase space density of ~ 0.1, the lowest order cumulant approximation is reasonable for present and likely also for future heavy-ion experiments. At the same time, the multi-boson effects can be important for realistic simulations of heavy ion collisions. As shown in ref. [18] (see also Section 5), for neutral pions they can lead to substantial distortions of the multiplicity distributions (increasing the original mean multiplicity by several tens per cent), of the single-pion spectra (enhancing production of the pions with low p_t and small $|y|$) and, to a lesser extent, of the two-pion correlation functions (the correlation function at a given multiplicity becoming lower and wider). For identical charged pions these effects are expected to be suppressed due to the repulsive Coulomb interaction.

4   Analytical model

To study the multi-boson effects in a dense pion gas we use a simple model assuming independent particle emission (see Eq. (11)) with the Gaussian ansatz for the single-boson emission function $D(p, x)$ [5]:

$$D(p, x) = \frac{1}{(2\pi r_0 \Delta)^3} \exp(-\frac{\mathbf{p}^2}{2\Delta^2} - \frac{\mathbf{r}^2}{2r_0^2})\delta(t). \tag{47}$$

Note that this ansatz corresponds to the independent one-particle sources of Kopylov and Podgoretsky, all of the same type, characterized by a universal size of $\sim 1/2\Delta$, with the centers distributed according to a Gaussian of a dispersion $\tilde{r}_0^2 = r_0^2 - (2\Delta)^{-2}$ (see Eq. (25)). Then, in the low density limit but regardless of the validity of the *smoothness* condition $\tilde{r}_0 \gg 1/2\Delta$ (see, however, the footnote after Eq. (31) concerning the independence assumption), the correlation function of two non-interacting identical particles measures the dispersion of the relative 4-coordinates $\tilde{x}$ of the centers of the one-particle sources as the inverse width squared of the correlation effect seen in the relative momenta $\mathbf{q} = \mathbf{p}_1 - \mathbf{p}_2$ [1]. For spin-0 bosons

$$R(\mathbf{p}_1, \mathbf{p}_2) = 1 + \langle \cos(q\tilde{x}) \rangle = 1 + \exp(-\tilde{r}_0^2 \mathbf{q}^2). \tag{48}$$

In this model the original boson phase space density (not affected by the BE effect) is given by

$$\tilde{f}_n(\mathbf{p}, \mathbf{x}) = \frac{n}{(r_0\Delta)^3} \exp(-\frac{\mathbf{p}^2}{2\Delta^2} - \frac{\mathbf{x}^2}{2r_0^2}). \tag{49}$$

The mean densities at a fixed boson momentum $\mathbf{p}$ and averaged over all phase space are

$$\langle \tilde{f}_n \rangle_{\mathbf{p}} \equiv \int d^3\mathbf{x}(\tilde{f}_n)^2 \ / \int d^3\mathbf{x}\tilde{f}_n = \frac{n}{(\sqrt{2}r_0\Delta)^3} \exp(-\frac{\mathbf{p}^2}{2\Delta^2}) \tag{50}$$

and

$$\langle \tilde{f}_n \rangle \equiv \int d^3\mathbf{x}d^3\mathbf{p}(\tilde{f}_n)^2 \ / \int d^3\mathbf{x}d^3\mathbf{p}\tilde{f}_n = n \ / \ (2r_0\Delta)^3, \tag{51}$$

respectively. Similarly, the original inclusive densities $\tilde{f}(\mathbf{p}, \mathbf{x})$, $\langle \tilde{f} \rangle_{\mathbf{p}}$ and $\langle \tilde{f} \rangle$ are given by Eqs. (49)-(51) with the multiplicity n substituted by the original mean multiplicity.

It is worth noting an approximate equality (see also a model independent prove in [7]) between the mean phase space density in the low density limit:

$$\langle \tilde{f} \rangle_{\mathbf{p}} = \frac{\eta}{(\sqrt{2}r_0\Delta)^3} \exp(-\frac{\mathbf{p}^2}{2\Delta^2}) \doteq \frac{\pi^{3/2}}{r_0^3} N(\mathbf{p}) \tag{52}$$

and the mean number of pions building the BE enhancement in the two-pion correlation function:

$$\int d^3\mathbf{q}[R(p_1, p_2) - 1]N(\mathbf{p}_1)N(\mathbf{p}_2)/N(\mathbf{p}) = \frac{\pi^{3/2}}{\tilde{r}_0^3} N(\mathbf{p}) \approx \langle \tilde{f} \rangle_{\mathbf{p}}, \tag{53}$$

$\mathbf{p}_{1,2} = \mathbf{p} \pm \mathbf{q}/2$. This equality is valid up to relative corrections $O((r_0\Delta)^{-2})$ and $O(\langle \tilde{f} \rangle_{\mathbf{p}})$, the latter representing an impact of the BE correlations on the single-boson spectrum (see Section 5.2).

It is important that the Gaussian ansatz in Eq. (47) allows to express the functions $G_n(\mathbf{p}_1, \mathbf{p}_2)$ and the integrals g_n (see Eqs. (28)) in simple analytical forms [15]:

$$\begin{aligned}
G_n(\mathbf{p}_1, \mathbf{p}_2) &= (2\pi\Delta^2 A_n)^{-3/2} \exp(-b_n^+(\mathbf{p}_1 + \mathbf{p}_2)^2 - b_n^-(\mathbf{p}_1 - \mathbf{p}_2)^2), \\
g_n &= (8\Delta^2 A_n b_n^+)^{-3/2},
\end{aligned} \tag{54}$$

where A_n, b_n^+ and b_n^- are given by the recurrence relations:

$$\begin{aligned}
A_n &= 2\Delta^2 A_{n-1}(b_{n-1}^+ + b_{n-1}^- + b_1^+ + b_1^-), \\
1/b_n^+ &= 1/(b_{n-1}^+ + b_1^+) + 1/(b_{n-1}^- + b_1^-), \\
b_n^- &= b_1^+ b_1^- / b_n^+,
\end{aligned} \tag{55}$$

with $A_1 = 1$, $b_1^+ = 1/(8\Delta^2)$ and $b_1^- = r_0^2/2$. The recurrence relations of this type allow for the analytical solution [17]. In our case it reads as:

$$b_n^+ = b_1^+ \epsilon^{-1}(1 - \rho^n) / (1 + \rho^n), \quad A_n = \beta^{2n/3} \epsilon(1 - \rho^{2n}), \quad g_n = \beta^{-n}(1 - \rho^n), \tag{56}$$

where $\epsilon^{-1} = 2r_0\Delta$, $\rho = (1 - \epsilon)/(1 + \epsilon)$ and the parameter

$$\beta = (r_0\Delta + 1/2)^3 \tag{57}$$

can be considered as a characteristic phase space volume.

For example, for $n = 2$ and 3, we have: $A_2 = (1 + \epsilon^{-2})/2$, $A_3 = (1 + 3\epsilon^{-2})^2/16$, $b_2^+ = 2b_1^+/(1 + \epsilon^2)$, $b_3^+ = 3b_1^+(1 + \epsilon^2/3)/(1 + 3\epsilon^2)$, $g_2 = \epsilon^3$, $g_3 = [4\epsilon^2/(3 + \epsilon^2)]^3$. Recall that the cumulants related to g_2 and g_3 are (see Eq. (30)) $K_2 = g_2$ and $K_3 = 2g_3$.

It follows from the recurrence relations (55) or their analytical solutions (56) that the slope parameters b_n^+ and b_n^- approach each other with increasing n. In the large-n ($n > r_0\Delta$) limit we then have [15]:

$$b_n^+ \to b_n^- \to r_0/(4\Delta), \quad A_n \to \beta^{2n/3} / (2r_0\Delta), \quad g_n \to \beta^{-n} \tag{58}$$

and

$$G_n(\mathbf{p}_1, \mathbf{p}_2) \to \beta^{-n} \left(\frac{r_0}{\pi\Delta}\right)^{3/2} \exp\left(-\frac{r_0}{4\Delta}(4\mathbf{p}^2 + \mathbf{q}^2)\right). \tag{59}$$

In very large-n ($n > e\beta$) limit, using the large-n behavior of the parameters g_n, we can get from the recurrence relation (31) the following behavior of the BE weight [15]:

$$\omega_n \to c(\beta)n! / \beta^n, \tag{60}$$

11

where $c(\beta)$ is a function factorially increasing with β, $c(1) = 1$.[5]

It is worth noting that the large-n limits become equalities at $\beta = 1$ $(r_0\Delta = 1/2)$ when $g_n = A_n = 1$, $K_n = (n-1)!$, $\omega_n = n!$ and $b_n^- = b_n^+ = r_0/(4\Delta)$. Recall that $\beta = 1$ corresponds to the minimal possible phase space volume when all the particle emitters are situated at one and the same space-time point so that the size $1/2\Delta$ of the elementary source determines not only the width of the single-particle spectrum but also the characteristic distance between the production points (see however the footnote after Eq. (31) and also ref. [18] for a more detailed discussion). In such a case $\tilde{r}_0 = 0$ and the correlation function equals 2 for any value of $\mathbf{q}$.

In the low-n $(n < r_0\Delta)$ limit, $i.e.$ in the case of a large phase space volume, it follows from Eqs. (55) or (56) that the slope parameter b_n^+ increases linearly with n up to the corrections $O((2r_0\Delta)^{-2})$ and that, at $n > 2r_0\Delta$, this increase saturates at $r_0/(4\Delta)$. Similar behavior shows the parameter $A_n/\beta^{2n/3}$. Thus, at $n \ll 2r_0\Delta$, we have:

$$b_n^+ = b_1^+ b_1^- / b_n^- \doteq n b_1^+, \quad A_n \doteq n(r_0\Delta)^{2(n-1)}, \quad g_n \doteq n^{-3}(r_0\Delta)^{-3(n-1)}. \tag{61}$$

Comparing the low-n approximations (61) for the parameters b_n^+, A_n and g_n with the large-n ones in Eqs. (58), we can see that they tail each other at $n = 2r_0\Delta$, $r_0\Delta/2$ and $r_0\Delta$ respectively. Correspondingly, the low-n approximation for the G_n-function

$$G_n(\mathbf{p}_1, \mathbf{p}_2) \doteq r_0^3 (r_0\Delta)^{-3n}(2\pi n)^{-3/2} \exp(-\mathbf{p}^2 n/2\Delta^2 - \mathbf{q}^2 r_0^2/2n) \tag{62}$$

tails with the large-n one in Eq. (59) at $1/2 < n_t/(r_0\Delta) < 2$.

Consider now the correlation function R_n defined in Eq. (40). To determine the normalization constant c_n, it is convenient to rewrite the single- and two-boson spectra at a fixed multiplicity n as

$$N_n^{(1)}(\mathbf{p}) = \sum_{j=0}^{n-1} \frac{\omega_{n-1-j}/(n-1-j)!}{\omega_n/n!} G_{j+1}(\mathbf{p}, \mathbf{p}) \equiv \sum_{j=0}^{n-1} \frac{w(n-1-j)}{w(n)} \widetilde{G}_{j+1}(\mathbf{p}, \mathbf{p}),$$

$$N_n^{(2)}(\mathbf{p}_1, \mathbf{p}_2) = \sum_{j=0}^{n-2} \frac{\omega_{n-2-j}/(n-2-j)!}{\omega_n/n!} \sum_{l=0}^{j} [G_{l+1}(\mathbf{p}_1, \mathbf{p}_1) G_{j-l+1}(\mathbf{p}_2, \mathbf{p}_2) + \\ G_{l+1}(\mathbf{p}_1, \mathbf{p}_2) G_{j-l+1}(\mathbf{p}_2, \mathbf{p}_1)] \tag{63}$$

$$\equiv \sum_{j=0}^{n-2} \frac{w(n-2-j)}{w(n)} \sum_{l=0}^{j} [\widetilde{G}_{l+1}(\mathbf{p}_1, \mathbf{p}_1) \widetilde{G}_{j-l+1}(\mathbf{p}_2, \mathbf{p}_2) + \widetilde{G}_{l+1}(\mathbf{p}_1, \mathbf{p}_2) \widetilde{G}_{j-l+1}(\mathbf{p}_2, \mathbf{p}_1)],$$

where $w(n)$, defined in Eq. (34), coincides with the BE affected multiplicity distribution arising from the Poissonian one characterized by the original mean multiplicity η and $\widetilde{G}_i(\mathbf{p}_1, \mathbf{p}_2) = \eta^i G_i(\mathbf{p}_1, \mathbf{p}_2)$. Noting further that b_n^+ approaches the limiting value $r_0/(4\Delta)$ from below, while b_n^- does it from above, we can see from Eq. (54) that, at large q, all terms in Eqs. (63) for $N_n^{(1)}(\mathbf{p}_{1,2})$ and $N_n^{(2)}(\mathbf{p}_1, \mathbf{p}_2)$ $(\mathbf{p}_{1,2} = \mathbf{p} \pm \mathbf{q}/2)$ can be neglected except for those containing the lowest slope b_1^+. For the normalization constant $c_n = \lim_{q \to \infty} [N_n^{(1)}(\mathbf{p}_1) N_n^{(1)}(\mathbf{p}_2) / N_n^{(2)}(\mathbf{p}_1, \mathbf{p}_2)]$ in Eq. (40) for the correlation function we thus get [15]:

$$c_n = [w(n-1)]^2 / [w(n)w(n-2)] \equiv n\omega_{n-1}^2 / [(n-1)\omega_n\omega_{n-2}]. \tag{64}$$

Regarding the (semi-)inclusive single- and two-boson spectra, they can be written in a form similar to Eqs. (63) only in the originally Poissonian case:

$$N^{(1)}(\mathbf{p}) = \sum_n \sum_{j=0}^{n-1} w(n-1-j) \widetilde{G}_{j+1}(\mathbf{p}, \mathbf{p}) / \sum_n w(n),$$

---

[5] A good approximation is $c(\beta) \doteq \beta^{d(\beta)}$, $d(\beta) = a_1 + a_2\beta^{a_3}$, $a_1 = 0.617$, $a_2 = 0.621$ and $a_3 = 0.788$.

$$N^{(2)}(\mathbf{p}_1,\mathbf{p}_2) = \sum_n \sum_{j=0}^{n-2} w(n-2-j) \sum_{l=0}^{j} [\widetilde{G}_{l+1}(\mathbf{p}_1,\mathbf{p}_1)\widetilde{G}_{j-l+1}(\mathbf{p}_2,\mathbf{p}_2) +$$
$$\widetilde{G}_{l+1}(\mathbf{p}_1,\mathbf{p}_2)\widetilde{G}_{j-l+1}(\mathbf{p}_2,\mathbf{p}_1)] / \sum_n w(n). \quad (65)$$

The normalization constant in Eq. (41) for the (semi-)inclusive correlation function is then [15]:
$$c = [\sum_n w(n-1)]^2 / [\sum_n w(n) \sum_n w(n-2)]. \quad (66)$$

Clearly, in the completely inclusive case (when the sums include all n from 0 to ∞ and $\sum_n w(n-j) = 1$), we have $c = 1$ and

$$\langle n \rangle = \sum_{j=0}^{\infty} \widetilde{g}_{j+1} \equiv \widetilde{g},$$

$$N^{(1)}(\mathbf{p}) = \sum_{j=0}^{\infty} \widetilde{G}_{j+1}(\mathbf{p},\mathbf{p}) \equiv \widetilde{G}(\mathbf{p},\mathbf{p}),$$

$$N^{(2)}(\mathbf{p}_1,\mathbf{p}_2) = \sum_{j=0}^{\infty}\sum_{l=0}^{j}[\widetilde{G}_{l+1}(\mathbf{p}_1,\mathbf{p}_1)\widetilde{G}_{j-l+1}(\mathbf{p}_2,\mathbf{p}_2) + \widetilde{G}_{l+1}(\mathbf{p}_1,\mathbf{p}_2)\widetilde{G}_{j-l+1}(\mathbf{p}_2,\mathbf{p}_1)]$$

$$\equiv \widetilde{G}(\mathbf{p}_1,\mathbf{p}_1)\widetilde{G}(\mathbf{p}_2,\mathbf{p}_2) + \widetilde{G}(\mathbf{p}_1,\mathbf{p}_2)\widetilde{G}(\mathbf{p}_2,\mathbf{p}_1), \quad (67)$$

where $\widetilde{g}_n = \eta^n g_n$. For the correlation function we have [15]:

$$R(\mathbf{p}_1,\mathbf{p}_2) = 1 + \frac{\widetilde{G}(\mathbf{p}_1,\mathbf{p}_2)\widetilde{G}(\mathbf{p}_2,\mathbf{p}_1)}{\widetilde{G}(\mathbf{p}_1,\mathbf{p}_1)\widetilde{G}(\mathbf{p}_2,\mathbf{p}_2)}. \quad (68)$$

Thus, in the considered case of the originally Poissonian multiplicity distribution, the intercept $R(\mathbf{p},\mathbf{p}) \equiv R(0) = 2$ in agreement with the result generally valid for thermalized systems [8].

5 Results

5.1 Multiplicity distributions

We will consider here the multiplicity distribution (34) resulting due to the BE effect on the originally Poissonian one with the mean multiplicity η. In accordance with the large-n behavior of the BE weights in Eq. (60) it takes on the following limiting form at $n > e\beta$ [15]:
$$w(n) \to \mathrm{const}' \cdot \xi^n, \quad \xi = \eta/\beta. \quad (69)$$

The large-n behavior of the multiplicity distribution in Eq. (69) indicates that it approaches the BE one:
$$w_{\mathrm{BE}}(n) = \nu^n / (1+\nu)^{n+1}, \quad \nu = \xi/(1-\xi), \quad (70)$$

with the mean multiplicity ν.[6] This is demonstrated in Figs. 1 and 2. Thus, at $r_0 = 2.1$ fm and $\Delta = 0.25$ GeV/c, the BE effect transforms the original Poissonian multiplicity distribution with $\eta = 30$ (dotted curve in Fig. 1a) to the one with much higher mean and dispersion values (solid curve in Fig. 1a). The exponential tail expected for the BE distribution is clearly seen in Fig. 1b where the results are presented in logarithmic scale for $\eta = 10$, $\Delta = 0.25$ GeV/c and $r_0 = 1.5$ fm. The slope parameter b in the exponential fit $w(n) = \text{const} \cdot \exp(-bn)$ of this tail at large n should be, according to Eq. (69), only a function of the variable ξ: $b = -\ln(\xi)$. Such a scaling is demonstrated in Fig. 2a for various values of η, Δ and r_0. Note that $\xi = 0.95$ and 0.72 for Figs. 1a and 1b, corresponding to $b = 0.02$ and 0.27, respectively.[7]

It should be noted that the experimental data point to a moderate value of the density parameter ξ. Thus, taking 0.2 as an estimate of the inclusive phase space density at $\mathbf{p} = 0$ from AGS and SPS experiments and using Eq. (52), we get (see the last Section) $\xi \approx 0.4 - 0.5$.

Using Eq. (67) for $\langle n \rangle$ and tailing the large- and small-n approximations of the integrals g_n at $n_t = r_0\Delta$ (see Eqs. (54) and (62)), we can approximate the mean multiplicity as

$$
\begin{aligned}
\langle n \rangle &\doteq \left[1 + \tilde{\xi}/2^3 + \cdots + \tilde{\xi}^{n_t-1}/n_t{}^3 \right] \eta + \xi^{n_t} \nu \\
&\equiv \langle n \rangle_{\text{g}} + \langle n \rangle_{\text{c}},
\end{aligned}
\tag{71}
$$

where $\tilde{\xi} = \eta/(r_0\Delta)^3 > \xi$; the density parameters $\tilde{\xi}$ and ξ coincide at $r_0\Delta \gg 1$. At large phase space volumes, $(r_0\Delta)^3 \gg 1$, the two terms in Eq. (71) can be considered as contributions of the BE gas and BE condensate respectively. It can be seen that the condensate dominates on condition $\langle n \rangle > \beta$.

Note that in the rare gas limit $\tilde{\xi} \ll 1$, we have $\langle n \rangle \doteq \left[1 + \tilde{\xi}/2^3 \right] \eta \equiv \eta + K_2\eta^2$, i.e. the increase of the mean multiplicity is dominated by the contribution of the second order cumulant $K_2 = (2r_0\Delta)^{-3}$. The corresponding multiplicity distribution then becomes wider than the Poissonian one (see Eqs. (32), (34)): $w(n) = \text{const} \cdot (1 + C_2^n K_2)\eta^n/n!$.

In Fig. 2c we demonstrate the approach of the mean multiplicity $\langle n \rangle$ to the limiting scaling value $\nu = \xi/(1 - \xi)$, though only for ξ very close to the explosion point $\xi = 1$ ($\xi > 0.99$). Instead, in the region of $\xi < 0.9$ indicated by present experiments, we can see, in agreement with Eq. (71) an approximate ξ-scaling of the ratio $\langle n \rangle/\eta$ (Fig. 2b).

Note that the approximate ξ-scaling gives a possibility to overcome technical problems with factorially large numbers at high multiplicities. Thus some quantities can be calculated at small or moderate values of η or n and then rescaled to large ones provided the density parameter $\xi = \eta/\beta$ or $\xi_n = n/\beta$ is kept the same.

Since, in the realistic event generators, the multi-boson effects can be accounted for only in the lowest order cumulant approximation [18], it is instructive to study the satu-

---

[6]This is in accordance with the appearance of the Bose-condensate in a dense ideal Bose gas [24]. The fluctuations of the number of particles in the condensate are very large - they are described by the well-known Einstein formula for identical bosons in the same quantum state. The corresponding BE multiplicity distribution in Eq. (70) turns to the Reley one for very large mean multiplicities. This type of BE condensate should not be mixed up with the multi-boson coherent (laser) state in which the BE correlations are absent and the multiplicity distribution corresponds to the Poisson law.

[7]At the explosion point $\xi = 1$ the tail of the multiplicity distribution becomes a constant ($b = 0$) so that the mean multiplicity $\langle n \rangle$ would go to infinity provided that there are no energy-momentum constraints. Note that the corresponding critical original mean multiplicity $\eta_{cr} = \beta \equiv (r_0\Delta + 1/2)^3$ is close but different from that given in Eq. (9) of ref. [5].

ration of these effects with the increasing number N_{cum} of the contributing cumulants. In Fig. 3 we show N_{cum}-dependence of the ratio $\langle n \rangle / \eta$ of the BE affected mean multiplicity to the original one for different values of the density parameter ξ. For example, at $\xi = 0.8$ this ratio saturates at $N_{cum} \sim 10$ ($\sim 40\%$ increase of $\langle n \rangle$). At $N_{cum} = 4$, representing a practical limit due to the numerical problems [18], the effect is underestimated by $\sim 25\%$ ($\langle n \rangle / \eta \approx 1.3$ instead of 1.4). The situation is more optimistic for lower densities. Thus at $\xi = 0.5$ the effect ($\sim 15\%$ increase of $\langle n \rangle$) practically saturates at $N_{cum} = 4$.

5.2 Single-particle spectra

The influence of the BE effect on the single-boson spectrum for a given boson multiplicity n, can be seen from Eqs. (30)-(35), (37) and (54). At sufficiently large momenta, when the local density $\langle f_n \rangle_{\mathbf{p}}$ remains small even at large n, this spectrum is dominated by the contribution $\beta_n P(\mathbf{p})$, $\beta_n = n\omega_{n-1}/\omega_n$, of the original spectrum. In such a rare gas limit, $\xi_{n,\mathbf{p}} \equiv \xi_n \exp(-\mathbf{p}^2/2\Delta^2) \ll 1$, we can write (see Eqs. (30), (37) and (32)):

$$
\begin{aligned}
N_n(\mathbf{p}) &\doteq n\frac{\omega_{n-1}}{\omega_n}G_1(\mathbf{p},\mathbf{p}) + n(n-1)\frac{\omega_{n-2}}{\omega_n}G_2(\mathbf{p},\mathbf{p}) \\
&\doteq n[1 - (n-1)K_2]G_1(\mathbf{p},\mathbf{p}) + n(n-1)G_2(\mathbf{p},\mathbf{p}) \\
&\doteq nP(\mathbf{p}) + n(n-1)K_2[2^{3/2}P(2^{1/2}\mathbf{p}) - P(\mathbf{p})].
\end{aligned}
\tag{72}
$$

Otherwise, at large local densities, $N_n(\mathbf{p})$ is determined by the asymptotic large-density spectrum [15]:

$$
N_n(\mathbf{p}) \rightarrow n\left(\frac{r_0}{\pi\Delta}\right)^{3/2}\exp\left(-\frac{r_0}{\Delta}\mathbf{p}^2\right) \equiv nP_c(\mathbf{p}),
\tag{73}
$$

associated with the BE condensate and corresponding to the asymptotic (large-n) value $r_0/(4\Delta)$ of the slope parameters $b_n^{\pm}$. Note that $P_c(\mathbf{p})$ is normalized to unity and that, at $\beta = 1$, it coincides with the original distribution $P(\mathbf{p})$.

It is clear from Eqs. (59), (60) and (63) that for small momenta, $p < \Delta(r_0\Delta - 1/2)^{-1/2}$, the condensate regime in Eq. (73) settles on condition $\xi_n > e$. For larger momenta, we must take into account that the condensate contribution vanishes much faster than that of BE gas, thus leading to much stronger condition of the condensate dominance:

$$
\xi_n > (2r_0\Delta)^{-3/2}\exp[(2r_0\Delta - 1)p^2/2\Delta^2].
\tag{74}
$$

Similar to the fixed multiplicity case, the inclusive single-boson spectrum at small local densities tends to $\eta P(\mathbf{p}) \equiv \tilde{G}_1(\mathbf{p},\mathbf{p})$ and, at large ones, it approaches the asymptotic high-density spectrum (see Eq. (73)):

$$
N(\mathbf{p}) \rightarrow \langle n \rangle P_c(\mathbf{p}).
\tag{75}
$$

The transfer of the original spectrum to the high-density one is demonstrated for the inclusive distribution in Fig. 4a and, more clearly, for ξ closer to the explosion point $\xi = 1$, in Fig. 4b.[8]

---

[8]These results agree with those obtained in refs. [5, 6] (see also [8, 18] and references therein) except for a wrong conclusion [5] that the width of the narrow peak due to the BE "condensate" is of $1/r_0$.

15

Tailing the large- and small-n behavior of the G_n-functions at $n_t \sim r_0\Delta$ (see Eqs. (59) and (62)), we can approximate the inclusive single-boson spectrum in Eq. (67) as

$$N(\mathbf{p}) \doteq \left[1 + \tilde{\xi}_{\mathbf{p}} / 2^{3/2} + \cdots + \tilde{\xi}_{\mathbf{p}}^{n_t-1} / n_t^{3/2}\right] \eta P(\mathbf{p}) + \xi^{n_t} \nu P_c(\mathbf{p})$$
$$\equiv N_g(\mathbf{p}) + N_c(\mathbf{p}), \tag{76}$$

where $\tilde{\xi}_{\mathbf{p}} = (2\pi)^{3/2} \eta P(\mathbf{p})/r_0^3 \equiv \tilde{\xi}\exp(-\mathbf{p}^2 / 2\Delta^2)$. Clearly, for large phase space volumes, $(r_0\Delta)^3 \gg 1$, the two terms in Eq. (76) can be interpreted as contributions of the BE gas and BE condensate respectively. Like in the fixed multiplicity case, the condensate dominates on condition (74) with the substitution $n \to \langle n \rangle$ ($\xi_n \to \langle n \rangle / \beta$).

In Fig. 4 we compare the inclusive single-boson spectra with the approximate formula (76). A good agreement is obtained despite the calculations were done for not very large phase space volumes. Experimentally the effect of BE "condensate" was searched for at SPS CERN as a low-p_t enhancement, however, with rather uncertain results (see, *e.g.*, [25]).

It follows from Eq. (76) that for sufficiently large ($n_t = r_0\Delta \gg 1$) and not very dense ($\xi \ll 1$) systems, similarly to the ξ-scaling of $\langle n \rangle / \eta$ (see Fig. 2b), the ratio $N(\mathbf{p})/[\eta P(\mathbf{p})]$ scales with the local density parameter $\tilde{\xi}_{\mathbf{p}}$. It appeares that analogical scaling takes place also at fixed multiplicity n.[9] In Fig. 5 we show the ratio of the single-particle spectrum at fixed n to the dominant large-$\mathbf{p}$ contribution $\beta_n P(\mathbf{p})$ of the original spectrum calculated at $\mathbf{p} = 0$ as a function of ξ_n for various multiplicities n. An approximate ξ_n-scaling is seen up to ξ_n of the order of unity. At larger ξ_n this ratio approaches the condensate limit $(2r_0\Delta)^{3/2}\xi_n$ which no more scales with ξ_n (see the corresponding curves in Fig. 5b). What scales at large ξ_n is not the ratio of the two contributions but the ratio of their integrals, n/β_n, the limiting value of which is just equal to $\xi_n = n/\beta$ since, according to Eq. (60), $\beta_n = n\omega_{n-1}/\omega_n \to \beta$ for $n > e\beta$.

5.3 Correlation functions

It follows from Eqs. (40) and (54)-(64) that, for a given multiplicity n, the correlation function intercept $R_n(\mathbf{p}, \mathbf{p}) \equiv R_n(0)$ decreases and the correlation function width increases with the increasing n or decreasing momentum p, both corresponding to the increasing local density parameter $\xi_{n,\mathbf{p}}$.

In fact, for large local densities (see Eq. (74)), the condensate behavior is achieved (see the curves in Fig. 5b) and the correlation function tends to unity not only at large but also at small $\mathbf{q}^2$. Indeed, in this limit the normalization constant $c_n \to 1$ (see Eqs. (43) and (60)) and the nominator and denominator of the correlation function (40) consist of about the same number $\sim n^2$ of the condensate terms $(r_0/\pi\Delta)^3 \exp[-(4\mathbf{p}^2 + \mathbf{q}^2)r_0/2\Delta]$ (see Eqs. (59), (60) and (63)).[10] The well known [3, 4, 5] lowering and widening of the correlation function with the increasing multiplicity is demonstrated, in the considered model, in Fig. 6.

---

[9]In this case, due to the explicit dependence of the particle spectra on the complicated BE weights ω_n, there is no analytical approximation similar to Eq. (76).

[10]Of course, the absence of the correlation in the condensate limit at fixed multiplicity has nothing to do with the coherence effect which is absent in the considered model. See the footnote after Eq. (31) and the discussion of the inclusive correlation function which appears to be different from 1 at whatever large densities.

Note however that in the rare gas limit, $\xi_{n,\mathbf{p}} \ll 1$, the change of the form of the correlation function with the increasing density is rather weak. Thus, writing in this limit

$$N_n^{(2)}(\mathbf{p}_1, \mathbf{p}_2) \doteq n(n-1)\frac{\omega_{n-2}}{\omega_n}[G_1(\mathbf{p}_1, \mathbf{p}_1)G_1(\mathbf{p}_2, \mathbf{p}_2) + G_1(\mathbf{p}_1, \mathbf{p}_2)G_1(\mathbf{p}_2, \mathbf{p}_1)]$$

$$+ n(n-1)(n-2)\frac{\omega_{n-3}}{\omega_n}[G_1(\mathbf{p}_1, \mathbf{p}_1)G_2(\mathbf{p}_2, \mathbf{p}_2) + G_1(\mathbf{p}_1, \mathbf{p}_2)G_2(\mathbf{p}_2, \mathbf{p}_1)$$

$$+ G_2(\mathbf{p}_1, \mathbf{p}_1)G_1(\mathbf{p}_2, \mathbf{p}_2) + G_2(\mathbf{p}_1, \mathbf{p}_2)G_1(\mathbf{p}_2, \mathbf{p}_1)]$$

$$\doteq n(n-1)[1 - (2n-3)K_2]P(\mathbf{p}_1)P(\mathbf{p}_2)\left[1 + \exp(-\tilde{r}_0^2\mathbf{q}^2)\right]$$

$$+ n(n-1)(n-2)2^{3/2}K_2\{P(\mathbf{p}_1)P(2^{1/2}\mathbf{p}_2)\left[1 + \exp\left(-\tfrac{3}{4}\tilde{r}_0^2\mathbf{q}^2 + \frac{\mathbf{p}\mathbf{q}}{2\Delta^2}\right)\right]$$

$$+ P(\mathbf{p}_2)P(2^{1/2}\mathbf{p}_1)\left[1 + \exp\left(-\tfrac{3}{4}\tilde{r}_0^2\mathbf{q}^2 - \frac{\mathbf{p}\mathbf{q}}{2\Delta^2}\right)\right]\}, \qquad (77)$$

$\tilde{r}_0^2 = r_0^2[1 - (2r_0\Delta)^{-2}]$, we get for the correlation function intercept an n-independent value close to 2: $R_n(0) \doteq 2(1 - \epsilon_1)$. Here we have introduced the density parameter

$$\epsilon_j = j \cdot 2^{5/2}K_2\exp(-\mathbf{p}^2 / 2\Delta^2) \doteq 2^{-1/2}\xi_{j,\mathbf{p}}. \qquad (78)$$

It should be noted that the correlation function $R_n(\mathbf{q})$ becomes less than unity at intermediate q-values and approaches the limiting value of 1 from below. This behavior and also the related suppression of the intercept value is caused by the BE correlation effect on the single-particle spectra entering the denominator of the correlation function. Sometimes this distortion is corrected for by a special iterative procedure. Its result can be described by a simple low-$\mathbf{q}^2$ correction factor:[11]

$$R_n^{cor}(\mathbf{p}_1, \mathbf{p}_2) = (A_n - B_n\mathbf{q}^2)R_n(\mathbf{p}_1, \mathbf{p}_2). \qquad (79)$$

In the low density limit of our model, we have

$$A_n = 1 + \epsilon_{n-1}, \qquad B_n = \epsilon_{n-1}[1 - (\mathbf{p} / \Delta)^2\cos^2\psi] / 8\Delta^2, \qquad (80)$$

where ψ is the angle between the vectors $\mathbf{p}$ and $\mathbf{q}$. At small $\mathbf{q}^2$, the corrected correlation function (properly normalized to unity at large $\mathbf{q}^2$) is then

$$R_n^{cor}(\mathbf{p}_1, \mathbf{p}_2) \doteq 1 + \exp(-\tilde{r}_0^2\mathbf{q}^2) + \epsilon_{n-2}\left[1 + \exp\left(-\tfrac{3}{4}\tilde{r}_0^2\mathbf{q}^2\right)\right] \qquad (81)$$

and can be represented in the usual single-Gaussian form:[12]

$$R_n^{cor}(\mathbf{p}_1, \mathbf{p}_2) = 1 + \lambda_n\exp(-r_n^2\mathbf{q}^2),$$

$$\lambda_n = 1 + 2\epsilon_{n-2}, \qquad r_n^2 = \tilde{r}_0^2\left(1 - \tfrac{5}{4}\epsilon_{n-2}\right). \qquad (82)$$

---

[11]The iterative correction procedure is usually used for small-acceptance detectors triggered by the requirement of at least two identical pions in the detector. The mixed reference sample then differs from the product of the single-particle spectra, being much more influenced by the residual BE correlations. The residual correlations can substantially affect also single-particle spectra in the case of a small effective emission volume, e.g.., in e^+e^--collisions. There are also other reasons for the low-q^2 correction factor, like energy-momentum constraints or presence of dynamical correlations (e.g.., in jets) which are destroyed in the mixed reference sample. For this reason the correction factor similar to that in Eq. (79) is often introduced as a pure phenomenological one with $A_n = 1$ and B_n treated as a free parameter.

[12]Note that in [17] a similar parametrization was used for the uncorrected correlation function. This led to different estimates of the interferometric parameters λ_n and r_n in the considered model.

We see that with the increasing n the effective interferometric parameters λ_n and r_n respectively increase and decrease slightly, starting from the zero density values of 1 and $\tilde{r}_0$.

In the low-density limit, simple Eqs. (81), (82) or directly Eqs. (72) and (77) allow one to determine the radius parameter r_0 by fitting the correlation functions R_n^{cor} or R_n. At higher densities, however, there is no simple analytical expression for the correlation function R_n and the eventual fit would require the use of rather complicated Eqs. (63). Another possibility is still a simple single-Gaussian fit at sufficiently small q, giving the effective interferometric parameters $\lambda_n^{eff} < 1$ and $r_n^{eff} < r_0$, both vanishing with the increasing local density. The low-density radius r_0 and the density can then be determined comparing λ_n^{eff} and r_n^{eff} with the model predictions as functions of r_0 and Δ.

In Fig. 7 we show the intercept as a function of the multiplicity n and the local density parameter $\xi_{n,\mathbf{p}}$ for several values of the mean momentum: $p = 0$, 0.1, 0.2 and 0.4 GeV/c. As expected, the intercept is practically constant at low local densities (small n or high p). As condensate develops, the intercept sharply falls down. The sharpness of this drop is however less pronounced at higher momenta even if plotted as a function of the local density parameter $\xi_{n,\mathbf{p}}$. Clearly, this lack of density scaling is related to a strong decrease of the condensate contribution with the increasing momentum. In fact, for the momenta $p > \Delta(r_0\Delta - 1/2)^{-1/2}$ the low-density parameter $\xi_{n,\mathbf{p}}$ strongly overestimates the local density in the region of the condensate dominance (see Eq. (74)). To demonstrate the possibility of the observation of the condensate effect for soft pions produced in certain high multiplicity events not following the ordinary proportionality rule between the freeze-out phase space density and pion multiplicity, in Fig. 7 we indicate by the arrows the intercept values corresponding to $\xi_n = 3\xi = 1.5$ ($n \approx 3\langle n \rangle$).

In the inclusive case corresponding to the original Poissonian multiplicity distribution, the correlation function intercept is equal to 2 for any local densities (see Eq. (68)). At very large local densities the two-boson spectrum approaches twice the product of the single-boson ones (see Eqs. (59) and (67)) so that the inclusive correlation function tends to the limiting value of 2 even at rather large relative momenta. The corresponding increase of the width of the correlation function with the increasing density parameter ξ is demonstrated in Fig. 8.

Note that at high local densities both the nominator and denominator of the correlation function at small $\mathbf{q}^2$ are dominated, like in the case of a fixed multiplicity, by the universal condensate terms, there numbers being about $\langle n(n-1) \rangle$ and $\langle n \rangle^2$ respectively. The difference between the inclusive and fixed multiplicity correlation functions, $R \to 2$ and $R_n \to 1$, is due to the fact that at high densities the originally Poissonian multiplicity distribution approaches a much wider BE one, for which $\langle n(n-1) \rangle = 2\langle n \rangle^2$.

Using the approximate equations (59) and (62) for the G_n-functions, we can analytically follow the behavior of the inclusive correlation function for large systems ($(2r_0\Delta)^2 \gg 1$) at $q \to 0$. Thus the function $\widetilde{G}(\mathbf{p}_1, \mathbf{p}_2)$ determining the two-boson inclusive spectrum (see Eq. (67)) can be approximated as a sum of the BE gas and BE condensate terms:

$$\widetilde{G}(\mathbf{p}_1, \mathbf{p}_2) \doteq N_{\mathbf{g}}(\mathbf{p}) \exp(-\mathbf{q}^2 r_{\mathbf{g}}{}^2/2) + N_{\mathbf{c}}(\mathbf{p}) \exp(-\mathbf{q}^2 r_{\mathbf{c}}{}^2/2), \qquad (83)$$

where $r_{\mathbf{c}}{}^2 = r_0/(2\Delta)$ and

$$r_{\mathbf{g}}{}^2 \doteq r_0{}^2 \sum_{n=1}^{n_t} \tilde{\xi}_{\mathbf{p}}{}^n n^{-5/2} \Big/ \sum_{n=1}^{n_t} \tilde{\xi}_{\mathbf{p}}{}^n n^{-3/2}. \qquad (84)$$

18

Note that at low local densities ($\tilde{\xi}_{\mathbf{p}} \ll 1$) the effective radius $r_{\mathbf{g}}$ coincides with $\tilde{r}_0 \doteq r_0$. With the increasing local phase space density it slightly decreases. The maximal reduction factor of $1/\sqrt{2}$ is achieved for large ($r_0\Delta \gg 1$) and dense ($\xi \to 1$, $\mathbf{p} \to 0$) systems. Considering the limit $q \to 0$ and $r_0\Delta \gg 1$, we can neglect the q-dependence of the condensate term ($r_c \ll r_g$) and of the product of the single-particle spectra in the denominator of the correlation function and, using Eqs. (68) and (83), write

$$R(\mathbf{p}_1, \mathbf{p}_2) \doteq 1 + \exp\left(-\frac{N_{\mathbf{g}}(\mathbf{p})}{N_{\mathbf{g}}(\mathbf{p}) + N_{\mathbf{c}}(\mathbf{p})} r_{\mathbf{g}}^2 \mathbf{q}^2\right). \tag{85}$$

It follows from Eq. (85) that the condensate contribution leads to an additional reduction of the interferometric radius squared (defined as a low-$\mathbf{q}^2$ slope of the correlation function) as compared with the case of a pure BE gas. In the case of a dominant BE condensate the interferometric radius tends to zero whatever large is the geometric size of the system.

Note however that, due to the non-Gaussian character of the correlation functions at large phase space densities, their real width is determined by the large-$\mathbf{q}^2$ behavior which reads as:

$$R(\mathbf{p}_1, \mathbf{p}_2) \doteq 1 + \left(\frac{N_{\mathbf{c}}(\mathbf{p})}{N_{\mathbf{g}}(\mathbf{p})}\right)^2 \exp(-r_{\mathbf{c}}^2 \mathbf{q}^2). \tag{86}$$

Requiring $R(\mathbf{q}_{\text{eff}}) = 1 + 1/e$, we get for the corresponding effective radius squared:

$$r_{\text{eff}}^2 \equiv \mathbf{q}_{\text{eff}}^{-2} = r_{\mathbf{c}}^2 / \left\{1 + 2\ln[N_{\mathbf{c}}(\mathbf{p}) / N_{\mathbf{g}}(\mathbf{p})]\right\}. \tag{87}$$

Thus, compared with the vanishing of the low-$\mathbf{q}^2$ slope of the correlation function (as $(1 - \xi)$), the effective radius squared vanishes at large phase space densities much slower (as $1/|\ln(1 - \xi)|$) (see Fig. 8).

It should be noted that Eqs. (67) and (68) assume that the original Poissonian multiplicity distribution extends to any arbitrarily large number of bosons. In reality, however, this number is limited due to the finite available energy. It is therefore interesting to see how fast the semi-inclusive spectra approach the inclusive limit with the increasing number n_{max} of the included pions. In Fig. 9 we demonstrate the n_{max}-dependence of the semi-inclusive correlation functions for a fixed value of the density parameter $\xi = 0.95$ and, in Fig. 10 - the n_{max}-dependence of the correlation function intercepts for different ξ-values. We can see that the width of the semi-inclusive correlation function increases with the increasing n_{max}, while its intercept decreases at small n_{max}, reaching a minimum at $n_{max} \approx \langle n \rangle$, and then approaches the limiting value of 2 roughly as $\log n_{max}$. The inclusive behavior is practically saturated at a moderate number of the included pions $n_{max} = k\langle n \rangle$, where k increases with the density parameter ξ from about 3 at $\xi = 0.89$ to about 5 at $\xi = 0.99$.[13] It thus justifies the neglect of the energy-momentum constraintss in Eqs. (67) and (68) provided $\langle n \rangle \ll \sqrt{s}/m$, e.g., in the usual case of a logarithmic increase of the mean multiplicity with the c.m.s. energy $\sqrt{s}$. The situation can change in the case of very large and dense systems dominated by a soft condensate. Then the regime $\langle n \rangle \sim \sqrt{s}$ can settle, the energy-momentum constraints leading to the reduction of the maximal effective number of produced pions to $n_{max} \sim \langle n \rangle$ and, as a result, to the suppression of the measured inclusive correlation function. Clearly, such an eventual suppression has nothing in common with the coherence effect.

---

[13]This increase is related with the increasing condensate contribution which, for the ideal BE gas, is charecterized by very large multiplicity fluctuations.

6 Discussion and conclusion

We have illustrated an approximate scaling of multi-boson effects with the density parameters $\xi, \xi_n, \ldots$ (see, e.g., Figs. 2 and 5). It means that though our numerical results were obtained for typical AGS or SPS multiplicities of the order of tens or hundreds of pions, they are approximately valid also for higher multiplicities expected at RHIC or LHC energies.

The value of the density parameter ξ can be estimated with the help of Eq. (53) relating the phase space density in the rare gas limit with the integrated correlation function. Thus using the usual Gaussian parametrization for the correlation function in the longitudinally co-moving system (LCMS):

$$R(p_1, p_2) = 1 + \lambda \exp(-r_x^2 q_x^2 - r_y^2 q_y^2 - r_z^2 q_z^2), \tag{88}$$

where x, y ($\mathbf{y} \parallel \mathbf{z} \times \mathbf{p}$) and z denote the outward, sideward and longitudinal directions respectively and parametrizing the single-particle spectra as

$$N(\mathbf{p}) = \frac{dn}{dy} \frac{\exp(-(m_t - m)/T)}{2\pi T(T + m)m_t \cosh y}, \tag{89}$$

we arrive at the mean pion phase-space density

$$\langle f \rangle_{\mathbf{p}} = \frac{\lambda \pi^{3/2}}{V} N(\mathbf{p}) \cosh y = \lambda \frac{\sqrt{\pi}}{2} \frac{\exp(-(m_t - m)/T)}{VT(T + m)m_t} \frac{dn}{dy}, \tag{90}$$

where $V = r_x r_y r_z$ is the LCMS interference volume. For soft pions ($p_t \approx 0$ and $y \approx 0$) at SPS energies this quantity is typically ~ 0.2. Since this value is sufficiently small, we can compare it with the model phase space density in the rare gas limit $\langle \tilde{f} \rangle_{\mathbf{p}=0} \approx \eta/(\sqrt{2}r_0\Delta)^3$ (see Eq. (52)) and get $\xi \approx 0.4-0.5$. For such values of the density parameter our calculations point to rather small multi-boson effects in the ordinary events. These effects can show up however in the events containing sufficiently high density fluctuations. Particularly, the condensate effects could be seen in certain high multiplicity events (see, e.g., Fig. 7) in which the phase space volume $\sim (r_0\Delta)^3$ does not follow the increasing multiplicity (as it presumably does in the ordinary events) and remains sufficiently small to guarantee a nonvanishing factor $\xi^{r_0\Delta}$ determining the condensate size (see Eqs. (71) and (76)).

Since at present energies the LCMS interference volume V seems to scale with dn/dy the freeze-out of the pions occurs on average at approximately constant phase space density (see Eq. (90)). In the rare gas regime, based on the density scaling one can then expect about the same relative size of the multi-boson effects also at RHIC and LHC energies, up to a slight increase in ξ due to the vanishing of the finite-size corrections with the increasing phase space volume of the emitting system. At the same time, the growing phase space volume will lead to suppression of the average condensate contribution, determined by the factor $\xi^{r_0\Delta}$.

Considering the multi-boson effects in the low (BE gas) and the large (BE condensate) density limits, we have obtained simple analytical formulae accounting for the finite size of the phase space volume and allowing to follow the dependence of the mean multiplicities, single-boson spectra and two-boson correlation functions on the phase space density

20

parameters. In principle, these formulae provide a possibility to identify multi-boson effects among others. Particularly, the width of the low-p_t enhancement due to the BE condensation decreases with the size of the system as $r_0^{-1/2}$ and this narrowing makes the observation of the effect easier.

The results of the considered simple model should not be taken, however, too literally since:

a) due to its static character, the model does not explicitly account for the experimental indications on a constant freeze-out phase space density and the related expansion of the emission volume. The qualitative application of our model to heavy ion collisions is however possible in the limited regions of the momentum space. For example, the pions with a rapidity difference greater than about unity have to be considered as originating from different static sources;

b) the inclusive spectra at sufficiently high mean multiplicity are dominated by the condensate contributions of high multiplicities in both extreme cases of very narrow or very wide multiplicity distributions (compared with the Poissonian one) of the originally uncorrelated bosons. Thus the intercept of 2 of the inclusive correlation function in the Poissonian case is likely to be a maximal one. Since the original multiplicity distribution for pions from the effective static source can be in fact wider than the Poissonian one (*e.g.*, due to the fluctuations of the mean multiplicity), we can expect the intercept less than 2 not only for the correlation functions at fixed multiplicities but also for the inclusive ones;

c) when estimating the freeze-out phase space density from the experimental data, the multi-boson system is considered as a homogeneous medium. However, there can be large local density fluctuations (not present in the model) which can give rise to noticeable multi-boson effects even at a moderate value of the mean phase space density;

d) on the other hand, the multi-boson effects can be somewhat suppressed due to a possible violation of the factorization assumption in Eq. (11) or due to the lack of the reflection symmetry of the emission volume. In latter case the functions $G_n(\mathbf{p}_1, \mathbf{p}_2)$ are no more real;

e) for identical charged pions, the BE effects are also suppressed due to the Coulomb repulsion. Since this repulsion is important only in a weakly populated region of very small relative momenta, the suppression of the global BE weights ω_n is rather small. For example, for ω_2 this suppression, being about $(ar_0\Delta^2)^{-1}$, is usually less than one per mill. The Coulomb distortion of the global multi-boson effects is therefore negligible in the rare gas limit. Nevertheless, since the Coulomb repulsion destroys the formation of the condensates made up from positive and negative pions in the disjoint phase space regions, it can lead to noticeable differences between charged and neutral pions in dense systems. Particularly, we can expect a decrease of the charge-to-neutral multiplicity ratio with the increasing phase space density.

Because of large numbers of positive and negative pions produced in heavy ion collisions, one could also raise a question about importance of the Coulomb screening effects violating the standard two-body treatment of the correlations in the low density limit. There are however arguments showing that the screening will be of minor importance even at LHC [15] (see also [26]). Note that in the scenario with a constant phase-space density the corresponding Debye radius

$$r_D = [4\pi(\rho_+ + \rho_-)e^2/T]^{-1/2}, \tag{91}$$

where $e^2 = 1/137$ and $\rho_+ + \rho_-$ is the total density of charged pions in the configuration

space, will be also constant, up to a weak energy dependence due to the temperature T. Assuming that pions with a rapidity difference greater than unity come from spatially disjoint regions of phase-space, we can put [15]

$$\rho_+ = \left(\frac{\lambda}{(2\pi)^3}\right)^{1/2}\frac{dn_+/dy}{V} = \frac{\sqrt{2}}{\sqrt{\lambda}\pi^2}T^3\langle f_+\rangle_y \tag{92}$$

and obtain $r_D \approx 15$ fm at $\langle f_+\rangle_y \approx 0.1$ and $T \approx 200$ MeV/c ($r_D \sim 1/T$). Thus at LHC energies we can expect the characteristic distances between the pion production points comparable or larger than the screening radius r_D leading to a suppression of the usual two-particle Coulomb effects. In fact, two charged pions produced at a distance $r^* > r_D$ start to feel their Coulomb field only after some time when the density decreases to a value corresponding to Debye radius smaller than r^*. During this time the vector of the relative distance between the pion emission points increases approximately by [15]

$$\Delta \mathbf{r}^* = \frac{\mathbf{k}^*}{T}V^{1/3}\Big[\Big(\frac{r^*}{r_D}\Big)^{2/3} - 1\Big]. \tag{93}$$

Substituting $\mathbf{r}^*$ by $\mathbf{r}^* + \Delta\mathbf{r}^*$ in the argument of the Coulomb wave function, we can see however that the suppression of the Coulomb effect can be substantial only in the region of large relative momenta $k^* > T$ where the correlations due to QS and FSI are already negligible (see, e.g., [19, 27]).

In conclusion we summarize the results. The influence of the multi-boson effects on boson multiplicities, single-boson spectra and two-boson correlations, including an approximate scaling behavior of some of their characteristics with the phase space density, has been demonstrated using the analytically solvable Gaussian model. The approximate analytical formulae are given allowing to follow the dependence of these quantities on the phase space density parameters thus providing a possibility for the identification of the multi-boson effects among others. Though these effects are hardly to be observable in typical events of heavy ion collisions in present and perhaps also in future heavy ion experiments, they can show up in certain classes of events containing sufficiently high density fluctuations.

Acknowledgments

References

[1] M.I. Podgoretsky, *Fiz. Elem. Chast. Atom. Yad.* **20** (1989) 628 (*Sov. J. Part. Nucl.* **20** (1989) 266).

[2] M.I. Podgoretsky, JINR Report **P2-85-240** (1985).

[3] W. Zajc, *Phys. Rev.* **D35** (1987) 3396.

[4] W.N. Zhang *et al.*, *Phys. Rev.* **C47** (1993) 795.

[5] S. Pratt, *Phys. Lett.* **B301** (1993) 159.

[6] S. Pratt, *Phys. Rev.* **C50** (1994) 469.

[7] G.F. Bertsch, *Phys. Rev. Lett.* **72** (1994) 2349.

[8] Yu.M. Sinyukov, B. Lorstad, *Z. Phys.* **C61** (1994) 587.

[9] J. Barrette et al., *Phys. Rev. Lett.* **78** (1997) 2916.

[10] B. Jacak, Proc. Int. Workshop on Multiparticle Correlations and Nuclear Reactions, CORINNE II, Nantes, France, 1994 (ed. J. Aichelin and D. Ardouin, World Scientific, 1994) p. 3.

[11] M. Gazdzicki, *Nucl. Phys.* **A590** (1995) 197c.

[12] P. Degtyarenko et al., *Z. Phys.* **A350** (1995) 263.

[13] S.V.Akkelin, Yu.M. Sinyukov, *Phys. Lett.* **B356** (1995) 525.

[14] Yu.M. Sinyukov, B. Lorstad, V.A. Averchenkov, *Z. Phys.* **C49** (1991) 417.

[15] B. Erazmus et al., ALICE Internal Note 95-43, Geneva, 1995.

[16] W.Q. Chao, C.S. Gao, Q.H. Zhang, *J. Phys. G: Nucl. Phys.* **21** (1995) 847.

[17] T. Csorgo, J. Zimanyi, *Phys. Rev. Letters* **80** (1998) 916; J. Zimanyi, T. Csorgo, CU-TP-818/1997.

[18] N.S. Amelin, R. Lednicky, *Heavy Ion Physics* **4** (1996) 241; SUBATECH 95-08, Nantes 1995.

[19] R. Lednicky, V.L. Lyuboshitz, Proc. Int. Workshop on Particle Correlations and Interferometry in Nuclear Collisions, CORINNE 90, Nantes, France, 1990 (ed. D. Ardouin, World Scientific, 1990) p. 42; JINR report P2-546-92 (1992) 1; *Heavy Ion Physics* **3** (1996) 93.

[20] S. Pratt, *Phys. Rev. Lett.* **53** (1984) 1219; *Phys. Rev.* **D33** (1986) 1314.

[21] R. Lednicky, V.L. Lyuboshitz, M.I. Podgoretsky, *Yad. Fiz.* **38** (1983) 251; V.L. Lyuboshitz, *Yad. Fiz.* **53** (1991) 823.

[22] I.V. Andreev, R.M. Weiner, *Phys. Letters* **B253** (1991) 416; Yu.M. Sinyukov, A.Yu. Tolstykh, ITP-92-5E, Kiev, 1992; *Z. Phys.* **C61** (1994) 593.

[23] J. D. Bjorken, Phys. Rev. **D27** (1983) 1327.

[24] L.D. Landau, E.M. Lifshitz, Statistical Physics: 2-nd Ed., Sect. 59, Pergamon Press, Oxford, 1969.

[25] Proc. of "Quark Matter 93", *Nucl. Phys.* **A566** (1994).

[26] D.V. Anchishkin, W.A. Zajc, G.M. Zinovjev, *Ukrainian J. Phys.* **41** (1996) 363.

[27] R. Lednicky, V.L. Lyuboshitz, *Yad. Fiz.* **35** (1982) 1316 (*Sov. J. Nucl. Phys.* **35** (1982) 770).
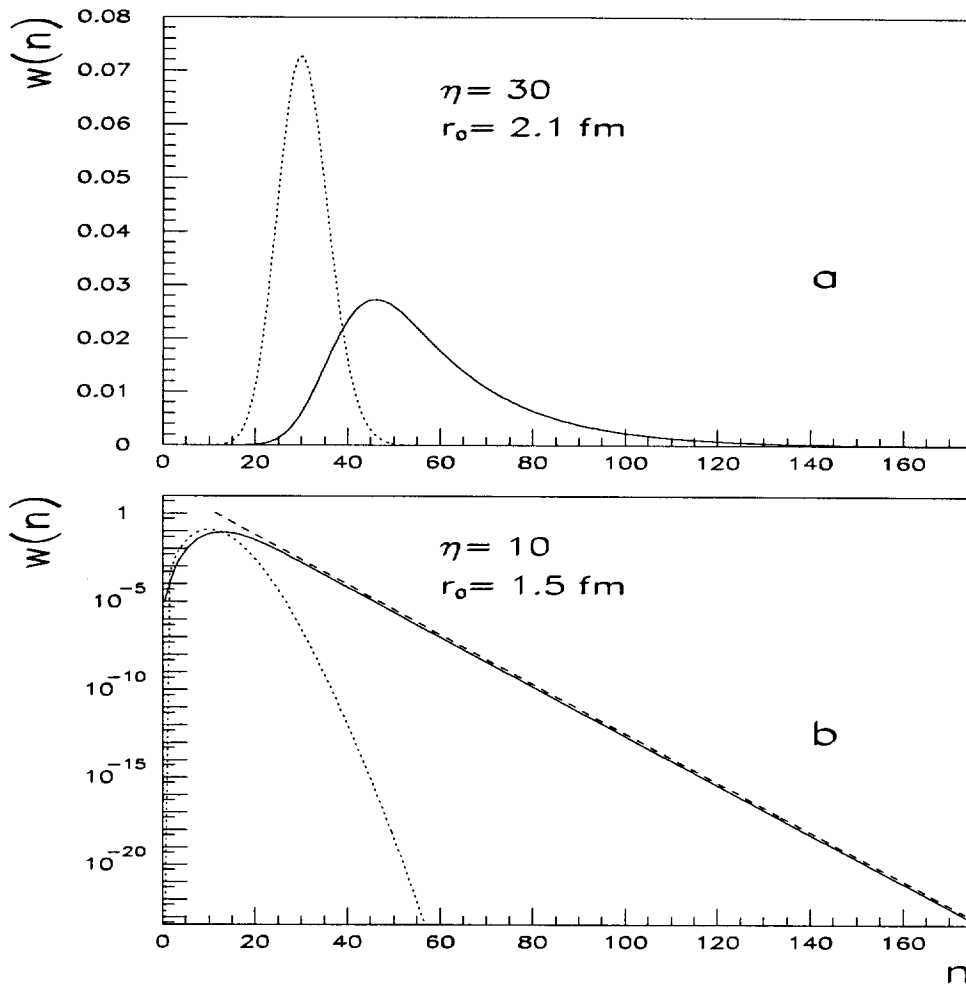
Figure 1: The multiplicity distribution of neutral pions for a) $\Delta = 0.25$ GeV/c, $r_0 = 2.1$ fm, $\eta = 30$ and b) $\Delta = 0.25$ GeV/c, $r_0 = 1.5$ fm, $\eta = 10$, where η is the mean multiplicity of the original Poissonian distributions (dotted curves).
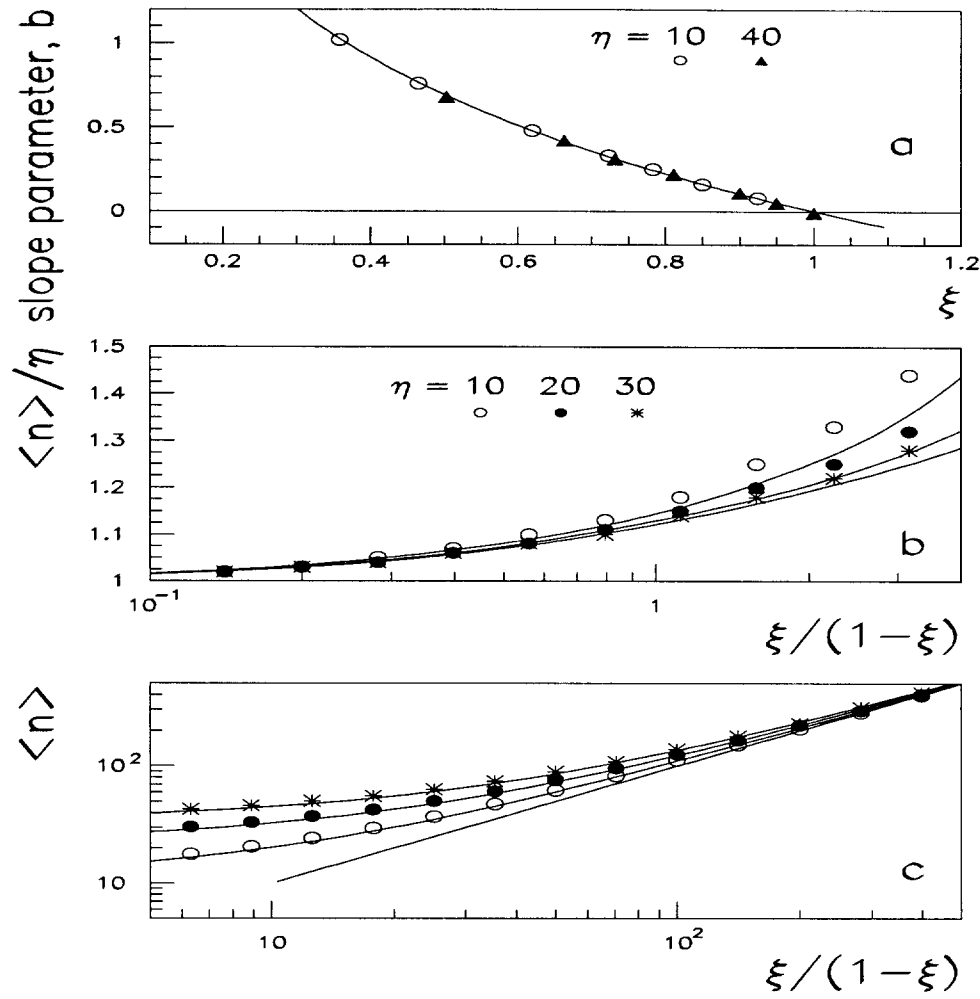
Figure 2: The slope parameter b of the exponential tail $c \cdot \exp(-b \cdot n)$ of the multiplicity distribution (a), the ratio of the mean multiplicity to the original Poissonian one (b) and the mean multiplicity (c) as functions of the density parameters $\xi = \eta/\beta$ and $\xi/(1 - \xi)$; $\Delta = 0.25$ GeV/c. The curve in (a): $b = -\ln\xi$, the curves in (b), (c) are calculated according to the tailing approximation in Eq. (71), the line in (c): $\langle n \rangle = \xi/(1 - \xi) \equiv \nu$.

26
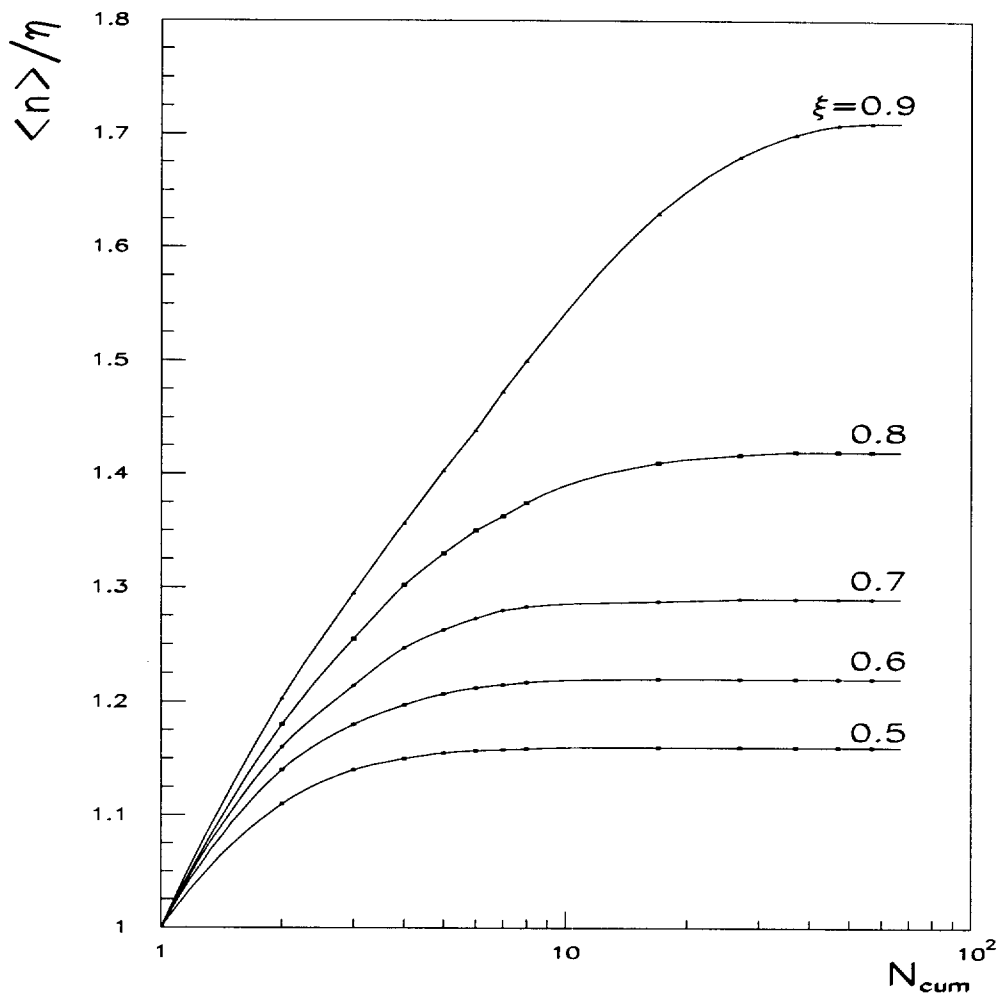
Figure 3: The ratio of the mean multiplicity to the original Poissonian one as a function of the number of the contributing cumulants for different values of the density parameter ξ.
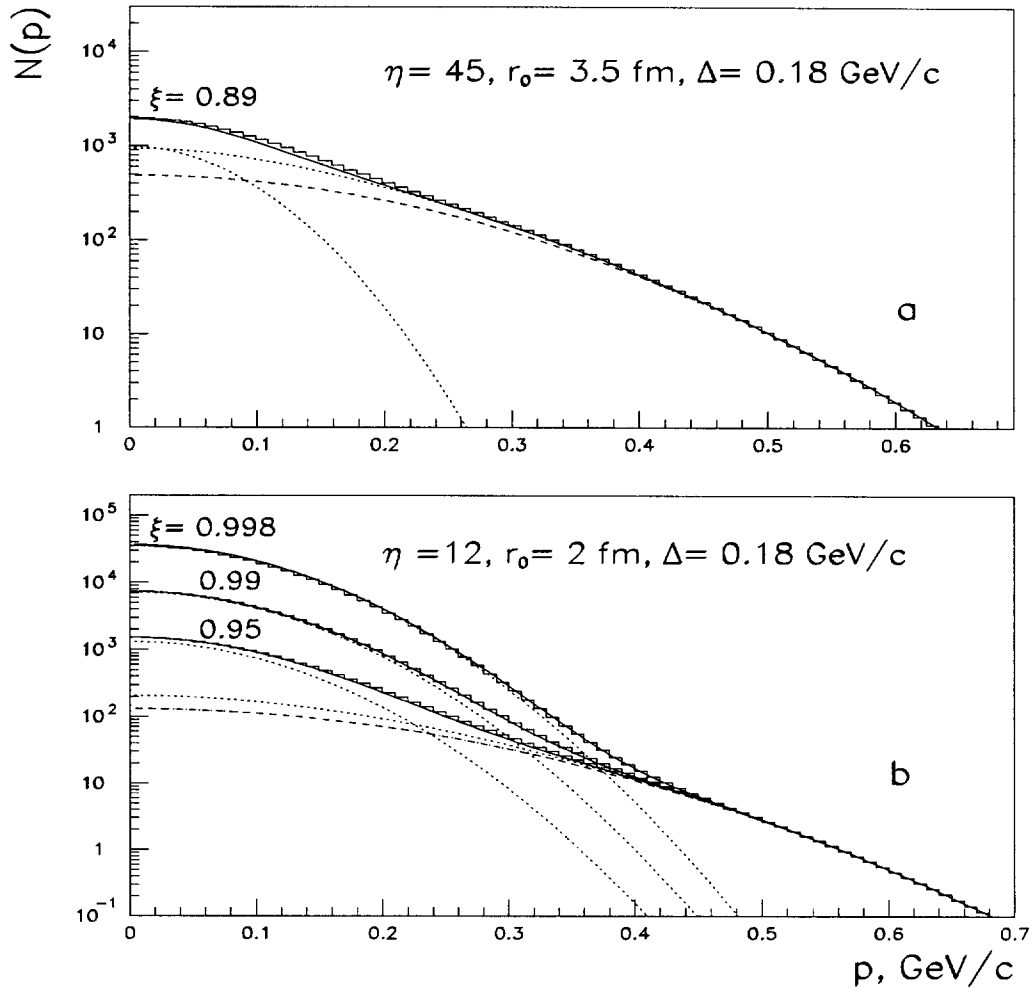
Figure 4: The inclusive single-particle spectra corresponding to the density parameters a) $\xi = 0.89$ and b) $\xi = 0.95$, 0.99 and 0.998 (the corresponding radius r_0 slightly varies near 2 fm). The full curves are calculated according to the tailing approximation (76), the dotted ones represent the contributions of the two (BE gas and BE condensate) terms in Eq. (76), the dashed curves, $\eta P(\mathbf{p})$, correspond to the rare gas limit.
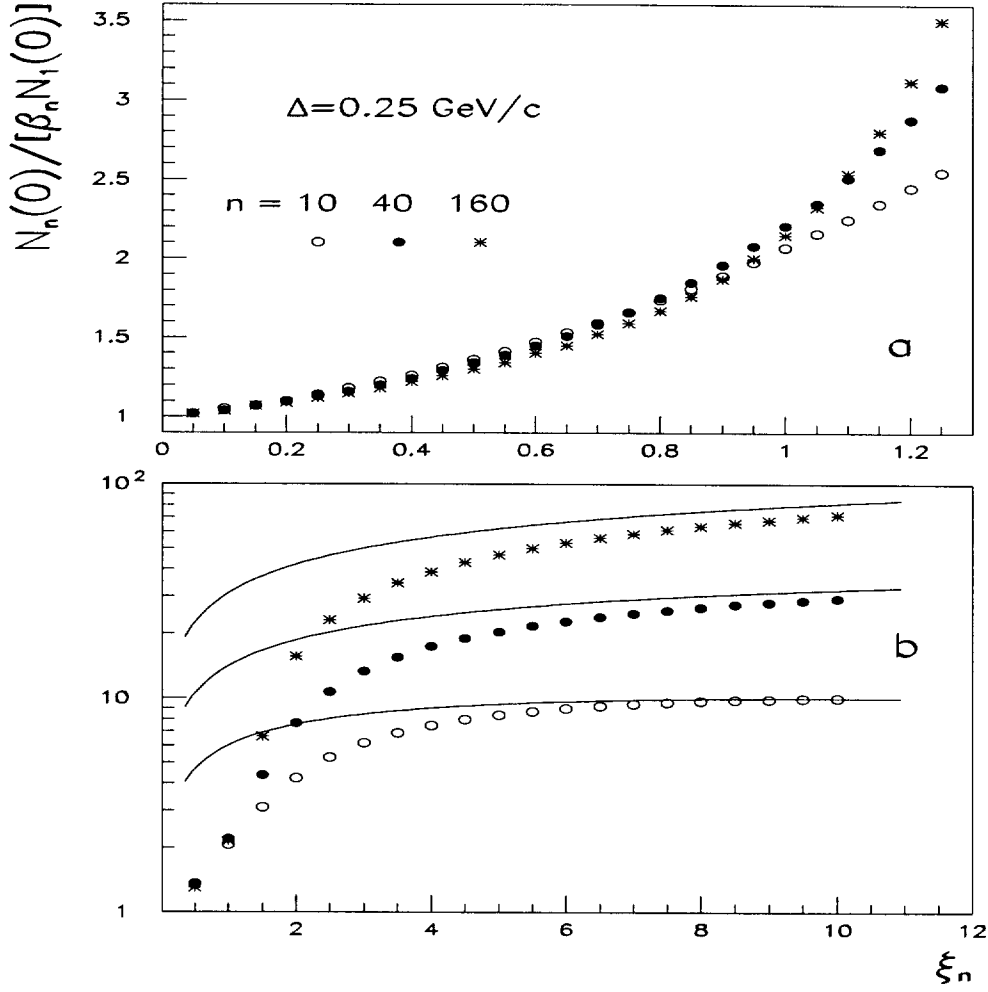
Figure 5: The ratios of the BE affected single-particle spectrum to the dominant large-$\mathbf{p}$ contribution $\beta_n N_1(\mathbf{p})$, $\beta_n = n\omega_{n-1}/\omega_n$, calculated at $\mathbf{p} = 0$ as functions of the density parameter $\xi_n = n/\beta$. The curves represent the large-ξ_n limit: $(2r_0\Delta)^{3/2}\xi_n \equiv [2(n/\xi_n)^{1/3} - 1]^{3/2}\xi_n$.
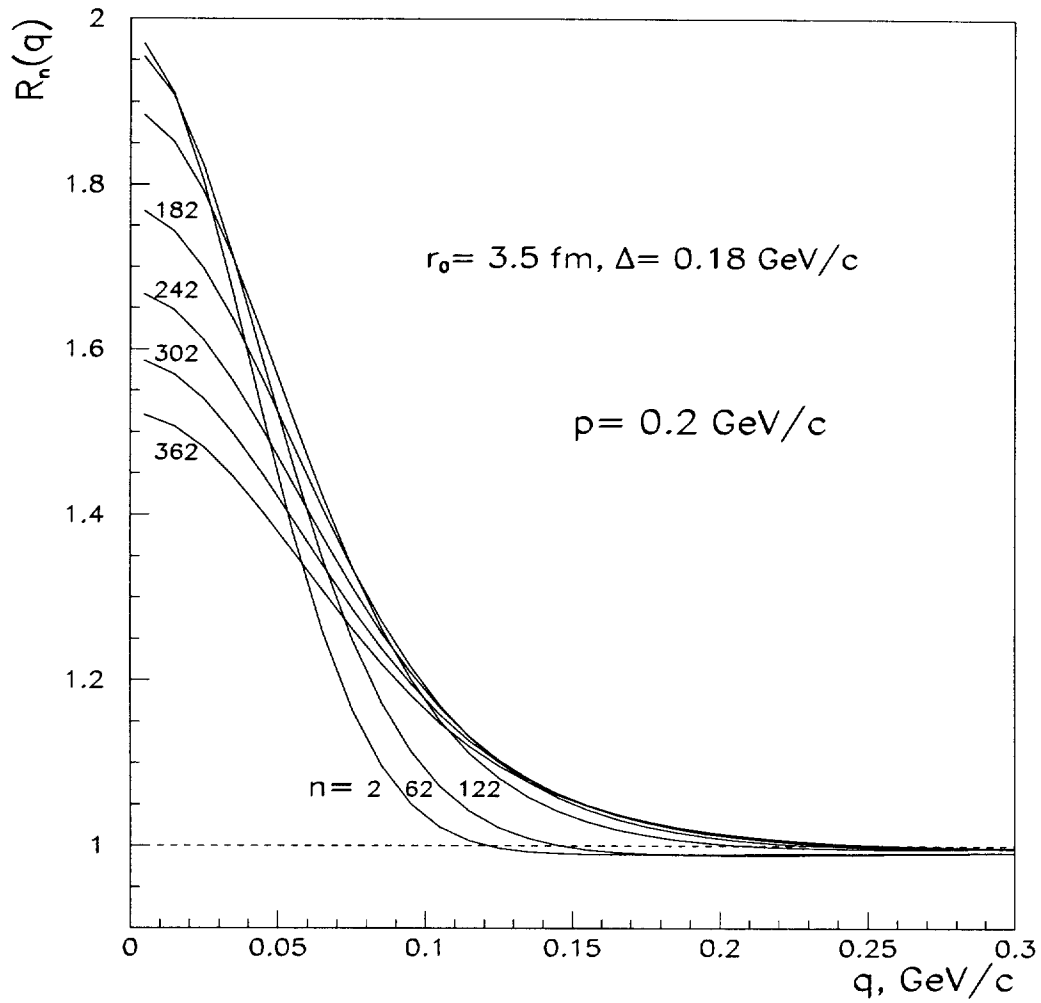
Figure 6: The two-pion correlation functions for the multiplicities increasing from $n = 2$ to 362 with a step of 60 (the corresponding density parameter ξ_n ranging from 0.04 to 7.2 with a step of 1.2). The higher is the multiplicity the lower is the intercept of the correlation function and the larger is its width.
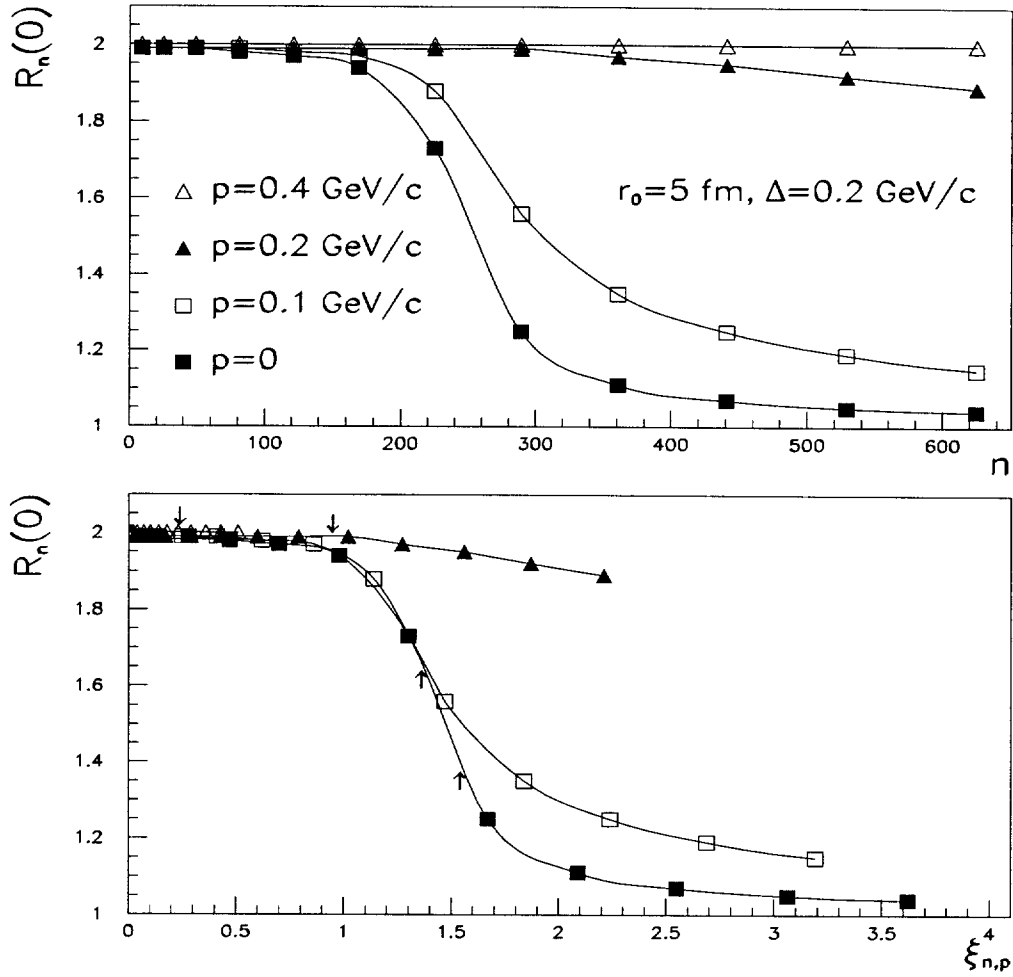
Figure 7: The intercept of the two-pion correlation functions as a function of the multiplicity n and the density parameter $\xi_{n,\mathbf{p}}$ for several values $p = 0$, 0.1, 0.2 and 0.4 GeV/c of the mean momentum of the two pions. The arrows on the interpolating curves indicate the intercept values corresponding to $\xi_n = 3\xi = 1.5$ ($n \approx 3\langle n \rangle$).
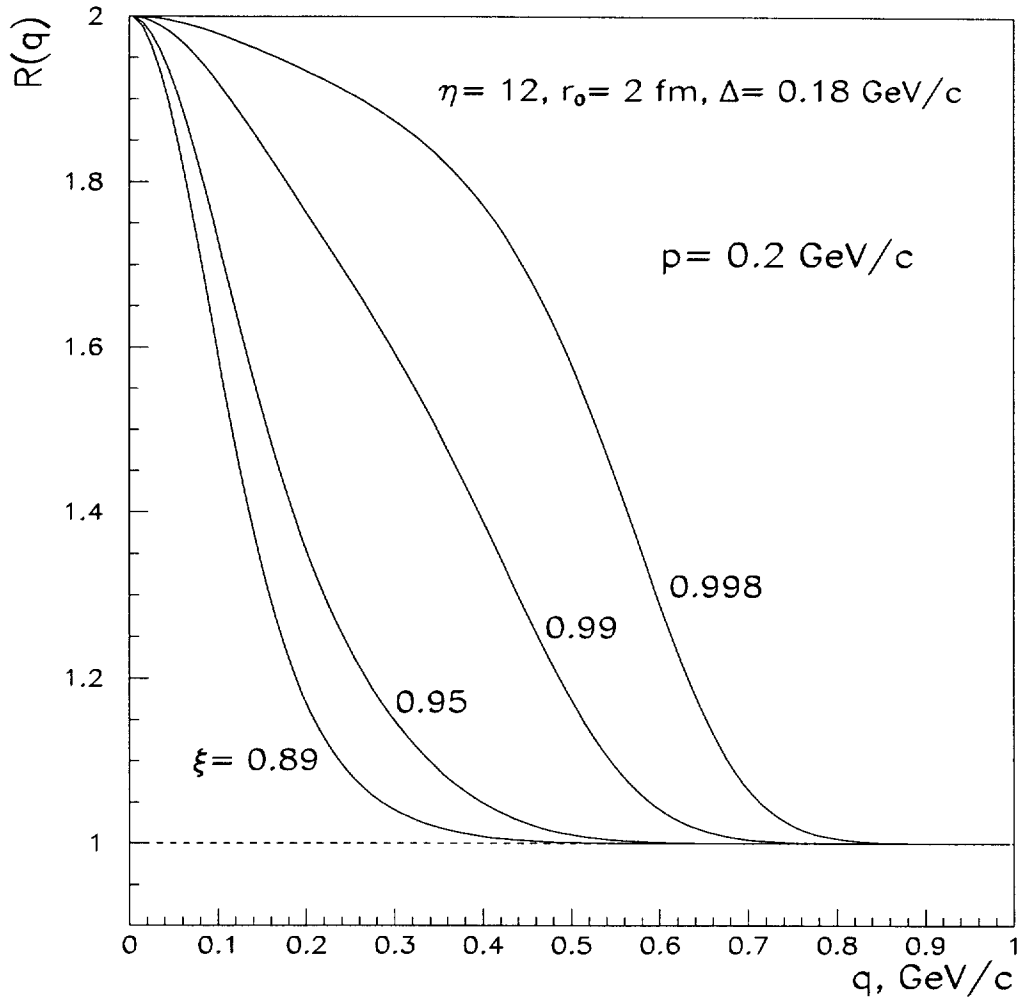
Figure 8: The inclusive two-pion correlation functions demonstrating the increase of the correlation width with the increasing density parameter ξ. The different ξ-values are achieved by slight variations of the radius r_0 around 2 fm.
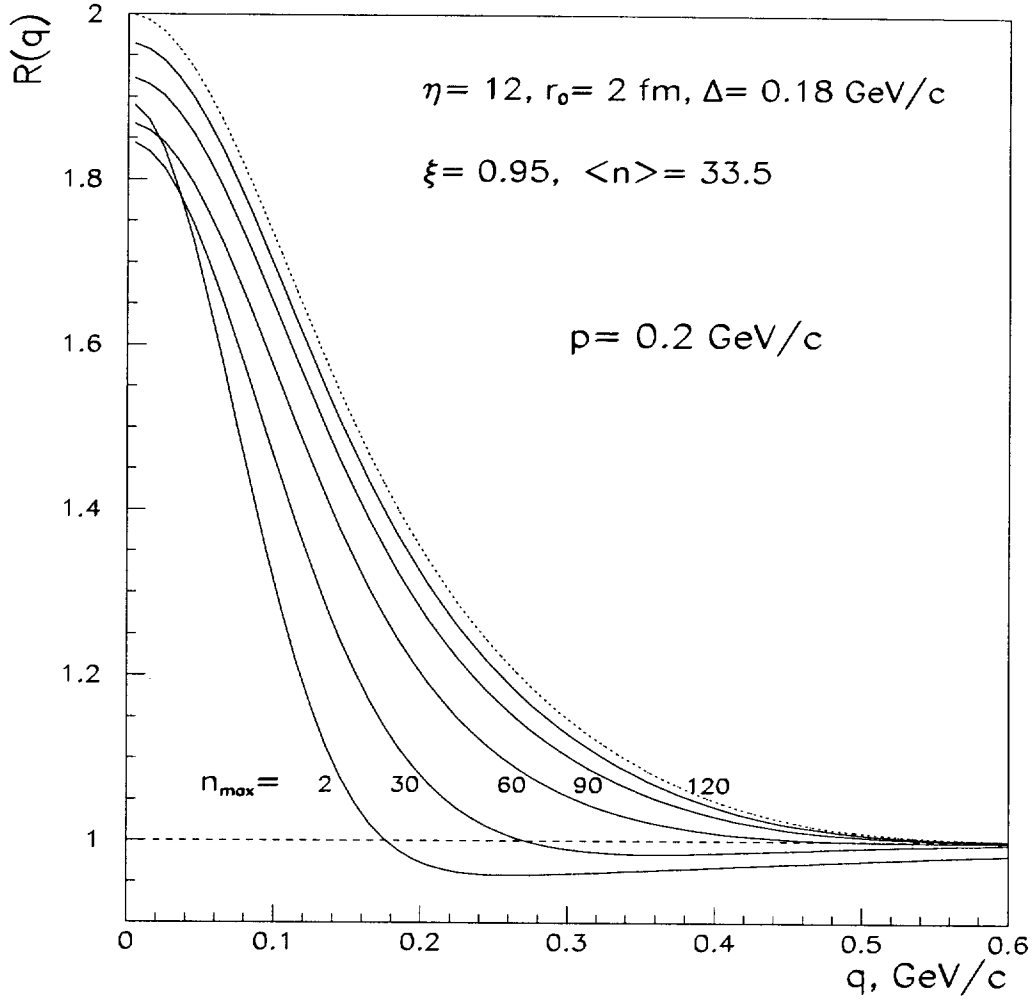
Figure 9: The semi-inclusive correlation functions including the pion multiplicities from 0 to n_{max} for different values of n_{max}. The dotted curve is the inclusive ($n_{max} \to \infty$) correlation function. The conditions are the same as in Fig. 8 for the density parameter $\xi = 0.95$.
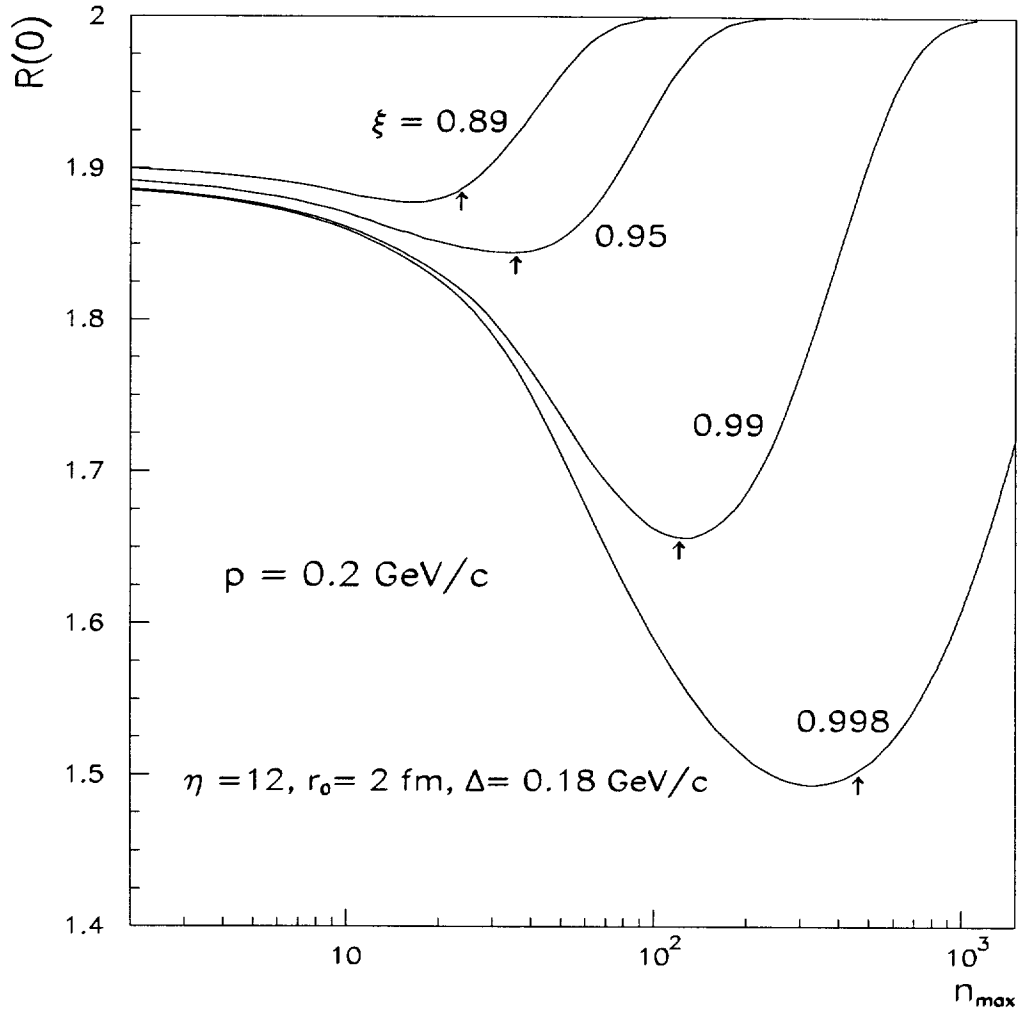
Figure 10: The intercepts of the semi-inclusive correlation function including the pion multiplicities from 0 to n_{max} as functions of n_{max} for different values of the density parameter $\xi = 0.89$, 0.95, 0.99 and 0.998; the arrows indicate the corresponding mean multiplicities $\langle n \rangle = 22.3$, 33.5, 113.7 and 433.8. The conditions are the same as in Fig. 8.